Agricultural and Forest Meteorology 378 (2026) 111003

Contents lists available at ScienceDirect

Agricultural and Forest Meteorology

journal homepage: www.elsevier.com/locate/agrformet

Projecting shifts in drought-induced thresholds for wheat yield loss under climate change in southeastern Australia

Keyu Xiang [a,b], Bin Wang [b,c,d,*], De Li Liu [b,d,e,*], Chao Chen [f], Fei Ji [g], Fangzheng Chen [h], Shijin Yao [a,b], Siyi Li [i], Alfredo Huete [a], Yi Li [j], Qiang Yu [k,*]

[a] Faculty of Science, School of Life Sciences, University of Technology Sydney, PO Box 123, Broadway, Sydney, NSW 2007, Australia
[b] NSW Department of Primary Industries, Wagga Wagga Agricultural Institute, Wagga Wagga, NSW 2650, Australia
[c] Hawkesbury Institute for the Environment, Western Sydney University, Richmond, NSW, Australia
[d] Gulbali Institute for Agriculture, Water and Environment, Charles Sturt University, Wagga Wagga, NSW 2650, Australia
[e] Climate Change Research Centre, University of New South Wales, Sydney, NSW 2052, Australia
[f] CSIRO Agriculture and Food, Private Bag 5, PO Wembley, WA 6913, Australia
[g] Science and Insights Division, NSW Department of Climate Change, Energy, the Environment and Water, Lidcombe, NSW 2141, Australia
[h] College of Land Science and Technology, China Agricultural University, Key Laboratory of Arable Land Conservation (North China), Ministry of Agriculture, Beijing, PR China
[i] School of Agriculture and Food Sciences, The University of Queensland, St Lucia, QLD, Australia
[j] College of Water Resources and Architectural Engineering, Northwest A&F University, Yangling, Shaanxi 712100, China
[k] State Key Laboratory of Soil Erosion and Dryland Farming on the Loess Plateau, Northwest A&F University, Yangling, Shaanxi 712100, China

ARTICLE INFO

Keywords:
Wheat yield
Drought threshold
APSIM
Conditional probability
Drought index
Climate change

ABSTRACT

Drought is a principal determinant of yield variability in rain-fed wheat systems, with climate change expected to exacerbate both the frequency and severity of water deficits. However, knowledge gaps remain in quantifying (i) yield loss probability across different drought indices and (ii) the dynamic thresholds at which drought induces yield losses under divergent climate scenarios. A systematic quantification of these relationships is essential to improve the empirical foundation for risk assessment and adaptive strategies in water-limited agricultural systems. This study analyses future wheat yield loss probability and dynamic drought thresholds in southeastern Australia using the APSIM model and copula functions, comparing a soil water index (SPAWI) against a precipitation index (SPI). We found a higher future wheat yield loss probability for SPAWI-based drought (5–20% greater than for SPI), underscoring the limitation of rainfall-only indices by neglecting soil buffer effects during drought. Drought thresholds were higher for SPAWI than SPI, due to soil moisture buffering, and lower in wetter regions. Including CO_2 fertilization increases yields and partially offsets drought impacts, lowering both loss probabilities and thresholds, while climate-model choice remains the dominant source of projected threshold shifts. Our analysis demonstrates that drought index selection influences yield-loss risk projections, and the quantified shifts in drought yield thresholds under climate change reveal key soil moisture buffering effects and CO_2 mitigation potential. These findings provide evidence-based drought thresholds to guide adaptive management in dryland wheat cropping systems under climate change.

1. Introduction

Drought can adversely affect crop production by increasing water demand (Mokhtar et al., 2021; Wan et al., 2021), resulting in significant yield reductions (Hao et al., 2024; Simanjuntak et al., 2023). As one of the driest countries (Wang et al., 2024b) and a major exporter of wheat production in the world (Li et al., 2024; Malik et al., 2022; Yuan and Yamagata, 2015), Australia faces significant challenges in maintaining the stability of its agricultural productivity under drought conditions. The New South Wales (NSW) wheat belt, accounting for about 35% of the national wheat output (https://www.agriculture.gov.au/abares), is particularly vulnerable to droughts. Additionally, a growing body of evidence indicates that climate change will further increase the frequency and duration of drought events in the future (Steensen et al.,

* Corresponding authors.
E-mail addresses: bin.a.wang@dpi.nsw.gov.au (B. Wang), de.li.liu@dpi.nsw.gov.au (D.L. Liu), yuq@nwafu.edu.cn (Q. Yu).

https://doi.org/10.1016/j.agrformet.2025.111003
Received 21 August 2025; Received in revised form 12 November 2025; Accepted 19 December 2025
Available online 3 January 2026

2025; Wu et al., 2025), consequently impairing crop development and amplifying yield instability (Li et al., 2022c; Wang et al., 2024b). Accordingly, accurate assessment of drought-induced yield losses is crucial for the timely detection of drought risk. However, research on wheat yield response to drought in Australia's wheat belt remains limited, particularly in future climate scenarios.

The complex nature of drought prevents its direct measurement (Hao and Singh, 2015; Mishra and Singh, 2010). Consequently, numerous drought indices have been developed to quantify drought severity (Mishra and Singh, 2011). Among these, standardized indices are the most widely used to systematically capture different drought types by converting drought-driving factors like precipitation, evapotranspiration, and soil water into standardized values (Chen et al., 2020; Liu et al., 2021; Mishra and Singh, 2010; Yerdelen et al., 2021). Commonly used indices include the SPI (McKee et al., 1993), SPEI (Vicente-Serrano et al., 2010), PDSI (Palmer, 1965), and SSI (Sheffield et al., 2004). Although single-index applications often perform well, selecting among different indices for a given application remains challenging (Barua et al., 2011; Farahmand and AghaKouchak, 2015; Wable et al., 2018). For instance, Tian et al. (2018) compared six drought indices in the south-central United States and found that their different calculation mechanisms can yield divergent assessments of drought conditions in the specific area. This discrepancy also extends to evaluations of drought impact on crop yield (Chen et al., 2020; Yao et al., 2022). For rainfed cropping systems, the primary factor affecting crop growth is water availability, which is directly influenced by precipitation and soil water storage capacity (Feldman et al., 2024; Miguez-Macho and Fan, 2021). Therefore, standardized indices based on these two variables can more accurately represent crop water stress. Furthermore, previous research, particularly on future climate projections, has predominantly relied on precipitation-based indices to characterize global drought patterns (Gebrechorkos et al., 2025; King et al., 2020). However, the water retention ability of soil can affect water supply to crops during precipitation deficits, and solely using precipitation-based indices may therefore introduce bias in assessing actual crop drought stress (Chen et al., 2024; Zhang et al., 2020). Hence, a quantitative comparison of different indices under future climate scenarios is necessary. Additionally, studies utilizing soil moisture-based indices to analyze future crop drought response remain limited, especially in drought-prone rainfed agricultural systems like the NSW wheat belt in Australia.

Previous studies have often linked standardized drought indices to crop yields through deterministic analytical approaches, such as linear regression and correlation analysis (Chen et al., 2020; Hendrawan et al., 2022). While these methods efficiently identify general relationships between drought trends and yield variation, they are generally unable to capture the dynamic responses of crop yield to evolving drought conditions. Moreover, drought is, by definition, a rare and slowly evolving phenomenon characterized by considerable spatial and temporal variability (Devanand et al., 2024; Hosseinzadehtalaei et al., 2024; Mishra and Singh, 2010). Its irregular onset, gradual progression, and nonlinear interactions with crop systems make it inherently difficult to capture using linear cause-and-effect assumptions (Clarke et al., 2021; Rahimi-Moghaddam et al., 2023). These constraints have motivated the shift toward probabilistic approaches that have been widely applied to quantify the risk of drought on wheat yield loss (Li et al., 2022b; Liu et al., 2022b). Recently, the concept of drought trigger thresholds has gained attention for dynamic analysis of drought impacts on specific crops (Wei et al., 2023b). In contrast to conventional deterministic methods, trigger thresholds based on drought indices identify the drought severity associated with the onset of yield loss, offering advantageous early-warning signals for agricultural risk management (Guo et al., 2023; Han et al., 2023). This method constructs joint probabilities between variables, typically involving a drought index, to determine drought trigger thresholds under fixed conditional probabilities (Huang et al., 2019; Li et al., 2022b). In addition, dynamic thresholds enable the incorporation of region-specific influencing factors in drought response (Li et al., 2022b; Xiang et al., 2023), leading to a more reliable estimation of drought impacts on wheat yield. For example, soil properties, in particular, play a critical role in buffering the effects of drought on crop growth (Boeing et al., 2022; Kukal et al., 2023; Zhao et al., 2023). To date, there has been limited research specifically focused on identifying drought thresholds and quantifying their potential changes under future climate scenarios in Australia. Moreover, under changing climatic conditions, it is essential to understand how these dynamic drought thresholds may shift in the future.

A robust evaluation of future drought effects on wheat requires both credible projections of drought evolution and reliable simulations of future yields (Asseng et al., 2014, 2019). Process-based crop models provide an appropriate platform to simulate crop growth and yields under specified scenarios by integrating data on climate, soil properties, cultivar characteristics, and management practices (Nóia-Júnior et al., 2025). In particular, Agricultural Production System sIMulator (APSIM) is extensively employed in Australia and performs well in local conditions (Holzworth et al., 2014). Nevertheless, integrated studies employing APSIM and drought trigger threshold analysis are notably lacking for the NSW wheat belt. Furthermore, yield projections are highly sensitive to climate input data, and the inherent uncertainties in the input from climate models introduce significant variability into these simulations (Li et al., 2023; Wang et al., 2020). In addition to more frequent droughts, rising CO_2 will affect wheat growth and yield. Although current understanding suggests a compensatory effect on C3 crop yields, such as wheat (Liu et al., 2022a; Sugiura et al., 2024), this

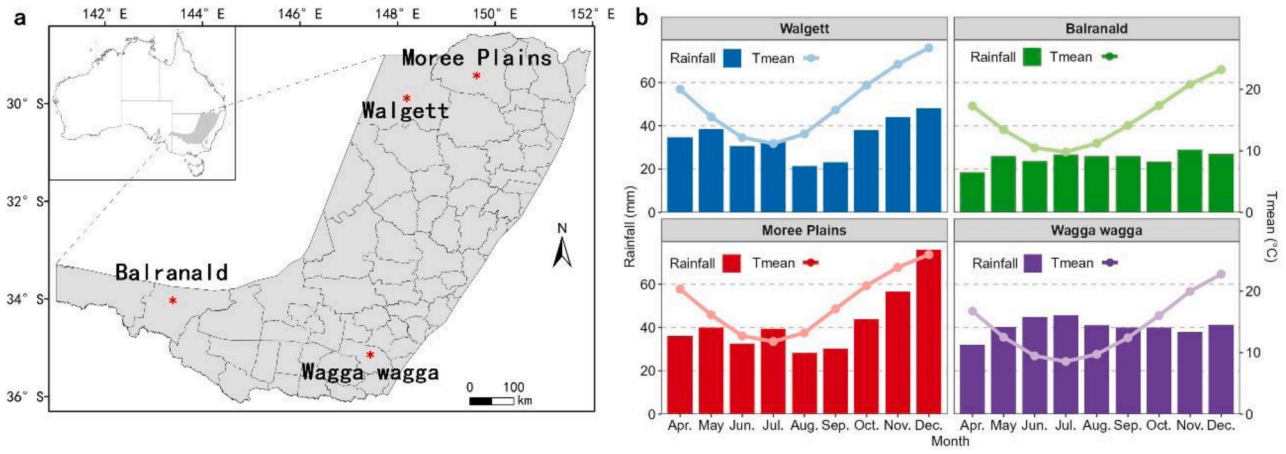

Fig. 1. The location of the NSW wheatbelt and the four selected sites (a). Mean monthly cumulative rainfall, average temperature (Tmean) during the wheat growing season (Apr. - Dec.) from 1981 to 2020 for the study sites (b).

benefit may be offset by concurrent drought stress (Rezaei et al., 2023; Wang et al., 2022b). How these interacting effects will operate under future climates, and how they will influence drought thresholds, remains unclear.

Therefore, this study integrates process-based crop modelling, joint and conditional probability methods, and uncertainty analysis to develop a framework for analysing the drought-induced threshold for yield loss under climate change. Wheat yield and soil available water were first simulated using historical and projected future climate data at four representative sites in southeastern Australia. A joint distribution function between the drought indices (SPI and Standardized Plant Available Water Index) and wheat yield was then constructed to identify thresholds using conditional probability methods. Finally, we evaluated threshold changes under climate scenarios and identified key contributing factors. The study aimed to 1) project the loss probability change of wheat yield with different drought indices under climate scenarios, 2) assess the change of drought-triggered yield loss threshold with two drought indices, and 3) identify the contributions to variations in drought-triggered thresholds for wheat yield loss. These findings will provide evidence-based drought threshold dynamics to inform adaptive management for rainfed wheat production systems in southeastern Australia.

2. Materials and methods

2.1. Study area and historical climate data sources

The NSW wheat belt is a vital region for Australian agriculture, primarily located in the central and western parts of New South Wales (Shi et al., 2023). This region experiences substantial climatic variability and geographic diversity, with annual rainfall in the west being up to four times lower than in the east, and annual temperature up to twice as high (Feng et al., 2019; Xiang et al., 2023). For this study, we selected four representative sites, Walgett (WA), Balranald (BA), Moree Plains (MP), and Wagga Wagga (WW) (Fig. 1a). The northern sites (WA and MP) are warmer, while BA in the west is drier, and WW in the east is wetter. They represent the main climate features of the wheat belt (Wang et al., 2017a). We utilized daily climate variables from the SILO dataset (Jeffrey et al., 2001). The daily data for the period 1981–2020, including maximum and minimum temperatures (°C), and rainfall (mm), were extracted to assess the impacts of climate variability and change on wheat yield in southeast Australia. The long-term means of monthly cumulative rainfall and monthly average temperatures across the selected sites during the wheat growing season (Apr. - Dec.) from 1981 to 2020 are shown in Fig. 1b.

2.2. Future climate data

Coupled Model Intercomparison Project version 6 (CMIP6) provides meteorological data for multi-model future climate projections (Hou et al., 2024; Wang et al., 2024b). Given the low resolution and biases in the raw GCM data (Table S1) (Li et al., 2025a), a statistical downscaling approach was applied to improve the accuracy of site-specific climatic data (Liu and Zuo, 2012). The approach involved spatial downscaling of the raw monthly weather data using inverse distance weighting, followed by bias correction. Daily weather data were then generated using the WGEN NWAI-WG weather generator (Liu and Zuo, 2012). This method for producing future weather data is widely used in climate change research (Sun et al., 2024; Zhang et al., 2023b).

Two Shared Socioeconomic Pathways (SSPs) were used in this study to represent different future climate scenarios: SSP2–4.5 (SSP245, intermediate scenario) and SSP5–8.5 (SSP585, high emissions scenario) (Li et al., 2024; O'Neill et al., 2016; Zhu et al., 2023). Although SSP585 is regarded as an "extreme" scenario (IPCC, 2021), exploring drought-triggered thresholds for wheat yield losses under such conditions is critical. Daily meteorological data downscaled from 27 GCMs were collected for the entire study period (1981–2100) under both SSP scenarios. The dataset included the same meteorological variables as the SILO dataset. To facilitate analysis and comparisons of variability, the period was divided into three intervals: present (1981–2020 is referred to as "Baseline"), near future (2021–2060, as "2040s"), and far future (2061–2100, as "2080s").

Table 1
Properties of soil for each study site.

Site	Soil ID	Layers	Depth (m)	PAWC[a] (mm)	Initial water[b] (%)
Walgett (WA)	Walgett No.1016	7	1.8	131	30
Balranald (BA)	Euston No.334	7	1.4	100	20
Moree Plains (MP)	Pallamallawa No.055	7	1.8	111	30
Wagga Wagga (WW)	Lockhart 2 No. 1085	9	1.8	144	50

[a] Plant available water capacity, the maximum amount of water the soil stores for plants.
[b] Percentage of maximum available water relative to the lower limit of the soil on the reset date.

2.3. APSIM-wheat simulation and validation

We used APSIM-Wheat, a widely recognized process-based crop model in Australia (Richetti et al., 2024; Wang et al., 2018), with version 7.10 to simulate multi-year wheat yields at study regions (Li et al., 2025b; Xiang et al., 2025). Moreover, the specific trial managements of the Grains Research and Development Corporation National Variety Trials (GRDC—NVT, https://nvt.grdc.com.au/) were used to adjust the simulation settings. Based on the sowing guide of GRDC, we selected the widely used cultivar "*Sunvale*" to simulate the wheat yield among all study sites (Feng et al., 2020a, 2019), with sowing depth and density set at 30 mm from the soil surface and 120 plants m^{-2}, respectively. The parameters of the cultivar are shown in Table S2. The initial nitrate-N and ammonium-N of the total soil layers were set to 35 kg ha^{-1} and 15 kg ha^{-1}, respectively, and another 60 kg ha^{-1} nitrogen fertilizer was added to the 50 mm depth from the soil surface on the sowing day. Sowing decisions were guided by a local empirical method within the sowing window and specific water requirements (Li et al., 2024; Xiang et al., 2025) (Eqs. (S1), (S2)). Corresponding representative soils were selected for each site from the APSoil database (Keating et al., 2003; Xiang et al., 2025), and detailed mechanical parameters of each soil are shown in Table 1. All the settings mentioned above were reset on the first day of each simulation year to remove the "carry-over" effects, which refers to the persistence of soil, crops, and management states from one growth season into the next (Wang et al., 2017b; Xiang et al., 2025), and the rest of the modules remained coherent to maintain consistency across simulations and ensure the wheat yields are mainly affected by climate change. Those settings were used in the simulations of the Baseline, 2040s, and 2080s. As the study objectives refer to the response quantification of wheat yield to drought impacts under future climate conditions, the simulated wheat yield, growth stage, and plant available water (PAW) were thus used for further analysis.

Although the APSIM-wheat model is widely employed and well-calibrated in Australia, specific tests are still essential for simulating results (Feng et al., 2020a). In this study, we collected the annual *in-situ* wheat yield data from the GRDC—NVT and the daily available water data from the Soil Moisture Integration and Prediction System (SMIPS) to validate the simulated wheat yield and PAW, respectively (Dreccer et al., 2018; Feng et al., 2022; Stenson et al., 2021). GRDC—NVT constitute Australia's largest independent multi-environment trial network for grain crops (https://nvt.grdc.com.au/). The framework

ensures consistent trial design and quality control, enabling robust comparisons of yield performance at site, regional, and seasonal scales (Feng et al., 2020a). SMIPS generates national daily total available soil water dynamics (0–90 cm) for plants across Australia at approximately 1 km resolution, and it is parameterised with physical properties from the Soil and Landscape Grid of Australia and employs a data-model fusion scheme driven by precipitation and potential evapotranspiration from the Australian Bureau of Meteorology (Stenson et al., 2021). We extracted site-matched annual yield of GRDC—NVT and daily available water of SMIPS using a nearest-neighbour criterion in latitude-longitude, and the matched records were then used for the validation of APSIM simulation. The coefficient of determination (R^2) and the root mean square error (RMSE) were used to assess the simulation performance (Feng et al., 2022; Quan et al., 2024), and the comparison results of the observed and simulated wheat yields and PAW are shown in Figs. S1 and S2, respectively.

The gradual rise in CO_2 is projected to substantially impact crop growth by modifying plant properties such as radiation use efficiency (RUE) (Feng et al., 2019). The effect of CO_2 on RUE in APSIM simulation is calculated by Eqs. (S3), (S4) (Ahuja et al., 2022; Zheng et al., 2015). We used empirical functions to generate the time-varying CO_2 concentrations under two SSP scenarios (Liu et al., 2014, 2017; Wang et al., 2022a) (Eqs. (1), (2)), and the atmospheric CO_2 was estimated based on the calendar year to represent "With CO_2" conditions. In addition to evaluating the impact of CO_2 on wheat yield and its effect on drought-trigger thresholds, we also included a controlled scenario with a constant CO_2 concentration of 412 ppm as "Without CO_2" conditions during the 2040s and 2080s based on measured CO_2 contents in 2020 (https://gml.noaa.gov/).

$$CO_{2,SSP245} = 62.044 + \frac{34.002 - 3.8702y}{0.24423 - 1.1542y^{2.4901}} + 2.6827 \times 10^{-4}(y-1960)^3 - 2.2448(y-2030) - 9.2751 \times 10^{-7}(y-1910)^4 + 2.8057 \times 10^{-2}(y-1900)^2 \quad (1)$$

$$CO_{2,SSP585} = 757.44 + \frac{84.938 - 1.537y}{2.2011 - 3.8289y^{-0.45242}} + 2.4712 \times 10^{-4}(y+15)^2 + 1.9299 \times 10^{-5}(y-1937)^3 + 5.1137 \times 10^{-7}(y-1910)^4 \quad (2)$$

where y is the calendar year from 2021–2100.

2.4. Standardized drought indices

In this study, APSIM simulation settings were held constant to isolate the climate factors, ensuring that crop growth was driven primarily by climatic variability rather than management interventions. Specifically, we examined wheat yield responses to drought, focusing on two types: meteorological drought, governed by precipitation anomalies (Feng et al., 2020b; Spinoni et al., 2019), and agricultural drought, represented by changes in soil water (Rahmati et al., 2020; Wu et al., 2025). Many standardized indices are available to represent drought severity, and multivariate approaches are often employed to increase accuracy (Mishra and Singh, 2011; Zargar et al., 2011). Nevertheless, when applied to future climate scenarios, the inclusion of additional climatic variables can introduce nontrivial uncertainty, as future climate model simulations already introduce heterogeneity (Virgilio et al., 2022; Yao et al., 2026). Additionally, indices that achieve higher reliability at extended time scales are poorly matched to the short-term drought dynamics governing crop growth (Geruo et al., 2017; Li et al., 2021). Therefore, we used the Standardized Precipitation Index (SPI) and Standardized Plant Available Water Index (SPAWI) to capture the meteorological and agricultural drought conditions during wheat growth.

Table 2
Severity categories of SPI and SPAWI.

Drought severity categories	Value range of SPI/SPAWI
Normal	(−0.5, 0]
Mild drought	(−1, −0.5]
Moderate drought	(−1.5, −1]
Severe drought	(−2, −1.5]
Extreme drought	(-∞, −2]

The SPI was chosen as a benchmark for precipitation deficit due to its computational simplicity and reliance solely on precipitation data (AghaKouchak and Hao, 2014; Dubois and Larocque, 2024; Wu et al., 2021). It is derived by transforming rainfall data into probability values through a gamma distribution and then is converted into standardized values using an inverse normal distribution (Angelidis et al., 2012; Kanthavel et al., 2022; Vergni et al., 2021; Yerdelen et al., 2021) (Eqs. (3), (4)). The SPAWI was selected as it directly reflects the soil water stress of crop growth by PAW and is a direct output of the APSIM soil water balance module (Gajurel et al., 2024; He and Wang, 2019; Verburg et al., 2017), ensuring mechanistic consistency within our modelling framework. SPAWI is constructed similarly to SPI, but it uses the empirical Gringorten plotting position formula for the distribution (Gringorten, 1963; Wu et al., 2021; Xiang et al., 2025, 2026) (Eq. (5)). The severity classification of SPI and SPAWI is shown in Table 2.

$$DI = \varphi^{-1}(p(x)) \quad (3)$$

$$p_{SPI}\left(x_i\right) = \frac{1}{\Gamma(\alpha)} \int_0^{\beta x_i} t^{\alpha-1} e^{-t} dt \quad (4)$$

$$p_{SPAWI}(x_i) = \frac{\#(x_j \le x_i) - 0.44}{n + 0.12} \quad (5)$$

where $\varphi^{-1}(*)$ is the inversed standard normal distribution function; x is the time series of rainfall or PAW, mm; $p(*)$ is the corresponding empirical probability of x_i; $\Gamma(*)$ is the Gamma function; α is the shape parameter; β is the rate parameter; n is the time series length of rainfall or PAW, i and j are the serial number of n, $1 \le j \le n$, and $i = 1, \ldots, n$; $\#(*)$ represents the rank of x in decreasing trend.

We adapted the calculation period to correspond with wheat growth stages. The end date of three wheat growth stages, including juvenile, flowering, and grain filling, was first identified based on the simulated phenological results from APSIM. For each stage, we used the end date as a reference and backcast a 30-day range, corresponding to “1 month”, to calculate monthly values, such as monthly cumulative rainfall and mean PAW. The adjusted data were then used to calculate the drought indices. In addition, 3-month and 6-month time scales were applied in the indices estimation, as previous studies indicated that longer time scales capture the drought impacts on crop yield effectively (Hendrawan et al., 2022; Peña-Gallardo et al., 2019; Xiang et al., 2023). So, there are 3 growth stages and 2 timescales of drought indices. For example, “SPI-3

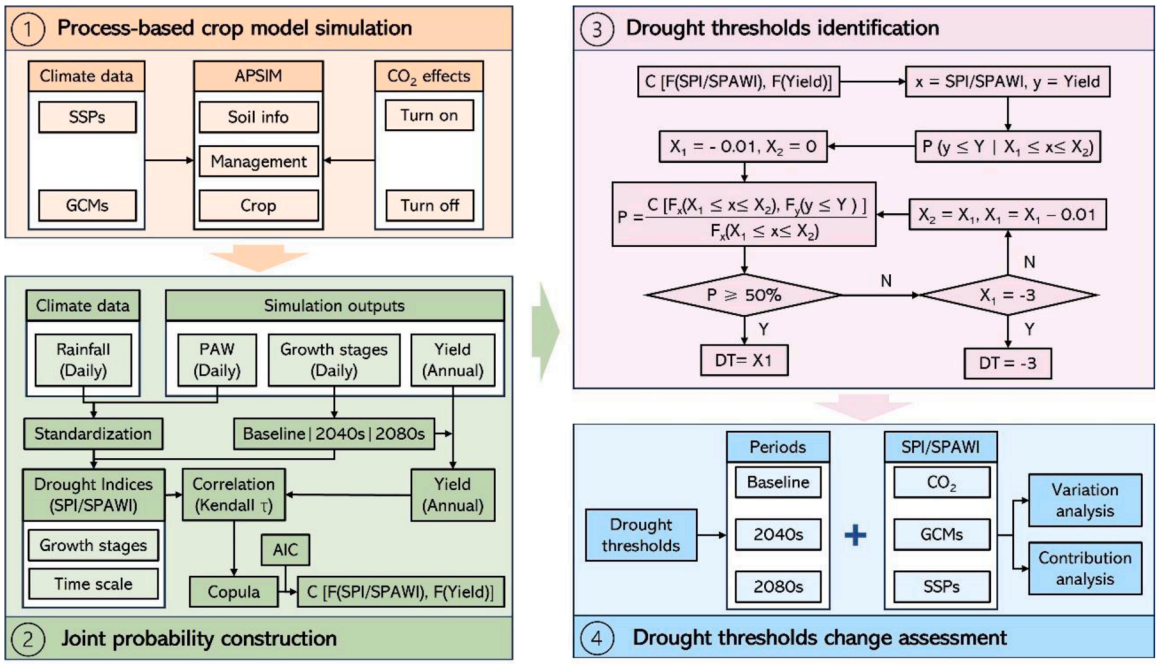

Fig. 2. Framework of yield loss probabilistic analysis and drought threshold identification. GCM, global climate model; SSP, shared socioeconomic pathways; APSIM, Agricultural Production System sIMulator; PAW, plant available water; AIC, Akaike Information Criterion; F(*), marginal cumulative distribution function; C(*), copula function; DT, drought threshold.

Juvenile" refers to the SPI value for the juvenile stage at the 3-month scale, and the same logic was applied to SPAWI.

2.5. Yield loss trigger threshold identification

Drought events disrupt wheat growth, reduce dry matter accumulation, and ultimately lead to yield declines (Gupta et al., 2020; Tardieu et al., 2018). To assess the severity of drought required to cause yield reductions, we applied a joint-conditional probability framework to identify the drought indices trigger threshold of wheat yield reduction. First, the time series of annual wheat yield and drought indices (SPI/SPAWI) were paired into corresponding sequences and then were assessed for correlation with Kendall's τ coefficient under different SSPs, GCMs, CO_2 conditions, and period intervals (Baseline, 2040s, and 2080s) (Temizhan et al., 2022). The drought index with the highest correlation coefficient was selected to construct a joint probability distribution and determine the drought-trigger threshold for yield reduction. Then, we fitted marginal distribution functions for the time series of yield and the corresponding drought index. Three distribution functions, Normal, Gamma, and Cauchy (Table S3), were used for wheat yield, and the Normal function was selected for drought index (Xiang et al., 2025). The marginal distributions of wheat yield and drought index were combined to construct the joint probability distribution functions by a two-dimensional copula method (Guo et al., 2023; Hao et al., 2017; Naseri and Hummel, 2022) (Eq. (6)), and five copula functions, including Clayton, Frank, Gaussian, Gumbel, and t (Genest and Favre, 2007) (Table S4) were applied to fit the optimal joint probability distribution functions between wheat yield and corresponding drought index based on the minimal value of Akaike Information Criterion (AIC) (Sakamoto et al., 1986), it represents the simultaneous occurrence of drought and yield reduction (Li et al., 2022b; Liu et al., 2022b).

Joint probability can be transformed into conditional probability to estimate the probability of wheat yield loss under specific drought conditions (Seo et al., 2024; Wei et al., 2023b; Zhang et al., 2023a) (Eq. (7)). We calculated the yield reduction risk as the conditional probability of simulated yields declining below the 20th percentile under specific drought conditions (SPI/SPAWI < -1). Additionally, as the drought index value decreases, the probability of yield falling below a set value approaches 100%. By fixing the conditional probability value, P_c, and the yield loss conditional value, Y_c, we can inversely determine the conditional drought index value that corresponds to a P_c likelihood of yield loss reaching Y_c. This value is referred to as the drought index trigger threshold of yield loss (*DT*) (Guo et al., 2023; Han et al., 2021) (Eq. (8)). In this study, we adopted the approaches from the previous research and set P_c at 50% and defined Y_c as the 30th of average yield simulated with SILO climatic data in the baseline period for each site (Han et al., 2023; Yang et al., 2024). The iteration range of the drought index was set from 0 to −3 based on the severity range (Table 2), with a step length of 0.01. When the conditional probability calculated from the iterated drought index exceeds the P_c, the *DT* is identified as the left side of this step interval (X_1 in Eq. (8)), and a detailed calculation procedure is shown in Fig. 2. Lower thresholds indicate the need for more severe drought conditions to cause the same yield loss (Han et al., 2023; Yang et al., 2024).

$$F_{x,y}(x,y) = C[F_x(x), F_y(y)] \tag{6}$$

$$P(y \le Y \mid x \le X) = \frac{P(y \le Y,\ x \le X)}{P(x \le X)} = \frac{C[Fy(Y),\ Fx(X)]}{Fx(X)} \tag{7}$$

$$P_c = P(y \le Y_c \mid x \le DT) = \frac{P(y \le Y_c,\ X_1 \le x \le X_2)}{P(X_1 \le x \le X_2)} = \frac{C[Fy(Y_c),\ Fx(X_2)] - C[Fy(Y_c),\ Fx(X_1)]}{Fx(X_2) - Fx(X_1)} \tag{8}$$

where x and y are the drought indices (SPI/SPAWI) and wheat yield, respectively; $F(*)$ and $C(*)$ are the marginal distribution function and copula function, respectively; X and Y are conditional values of SPI/SPAWI and wheat yield, respectively; P_c is the fixed conditional probability; Y_c is the fix conditional wheat yield; X_1 and X_2 are the left and right side value of drought index step interval.

2.6. Contribution analysis

We employed a three-way Analysis of Variance (ANOVA) to identify the contribution sources of variation in the drought index trigger threshold for yield reduction under future climate conditions (Huang et al., 2022; Li et al., 2025a; Wang et al., 2020). SSP, GCM, and CO_2 conditions were selected as contributing factors, and both the individual and interaction effects were analyzed (Eq. (9)).

$$SST = SS_{SSP} + SS_{GCM} + SS_{CO2} + SS_{SSP\times GCM} + SS_{SSP\times CO2} + SS_{GCM\times CO2} + SS_{SSP\times GCM\times CO2} \quad (9)$$

where SST is the total sum of squares of all factors; SS_{SSP}, SS_{GCM}, and SS_{CO2} are the separate contributions of SSP, GCM, and CO_2 conditions, respectively; $SS_{SSP\times GCM}$, $SS_{SSP\times CO2}$, $SS_{GCM\times CO2}$, and $SS_{SSP\times GCM\times CO2}$ are the interaction contributions of SSP, GCM, and CO_2 conditions.

2.7. Statistical test

We conducted several tests in the construction process of joint probabilities to ensure the data meet the fitting requirements. The Genest and Favre (2007) method was employed to evaluate the Kendall's τ correlation coefficient results. The Ljung-Box test was applied to assess autocorrelation in the time series of wheat yield and drought index (Ljung and Box, 1978), and the Kolmogorov-Smirnov test was used to test marginal distribution fitting results (Gunar and Trenkler, 1995). Finally, the goodness of fit for the copula function was assessed using White's information matrix equality (Huang and Prokhorov, 2014; White, 1982). The general framework of the study is shown in Fig. 2.

3. Results

3.1. Changes in wheat yields and drought indices

Fig. 3 illustrates the ensemble means of wheat growth stages under SSP245 and SSP585 scenarios for the baseline period, the 2040s and the 2080s. Fig. 3a presents the duration of each stage, while Fig. 3b depicts the earliest start and the latest end dates. In general, most sites experienced the longest duration at the juvenile stage, and the shortest in the grain filling stage. In the southern sites (BA, WW), the duration of growth stages was progressively shortening, with this trend expected to intensify in the future. For instance, under SSP245, the juvenile stage in WW shortened from 78 days during the baseline to 73 days in the 2080s, and decreased further to 72 days under SSP585. A similar pattern of substantial shortening was observed for the flowering stage across southern sites. Concurrently, the initiation of most growth stages advanced, particularly under SSP585. At WW, the flowering stage began 10 days earlier in the 2080s under SSP245 and 12 days earlier under SSP585, while grain filling commenced 14 and 18 days earlier, respectively. Spatially, MP consistently exhibited the earliest start dates across growth stages, followed by WA and BA, with WW starting the latest.

We compared projected wheat yields under different CO_2 conditions to the baseline, with results shown in Fig. 4a. Wheat yields declined when the CO_2 level remained constant, with greater decreases observed under SSP585 compared to SSP245. For instance, wheat yields in WW decreased by 17% in the 2080s under SSP585 (median reduction of 27 GCMs, applicable hereafter), compared to a 5% decline under SSP245. In WA, the yield decreases under SSP585 were −8% in the 2040s and −16% in the 2080s, while under SSP245, they were −15% and −15%, respectively. In contrast, under scenarios with continuous CO_2 increases, wheat yields at the northern station increased in the future, with SSP585 resulting in larger increases than SSP245. These increases were more pronounced in the 2080s. For example, MP yields decreased by 5% in the 2040s and 1% in the 2080s under SSP585, compared to 0 and 20% increases under SSP245.

We also analyzed the temporal changes in SPI and SPAWI across the entire period. The grain filling stage results at a 6-month scale are shown in Fig. 4b. Under both SSP245 and SSP585 scenarios, drought indices exhibited broadly similar temporal patterns, though variations existed across regions and drought indices. In southern sites (BA and WW), the SPI showed gradual declines over time. Similarly, the SPAWI in WW declined more sharply, while the SPAWI decreased marginally in BA. In contrast, northern regions displayed stable SPI trends (WA and MP), with median values hovering near baseline levels. In addition, the SPAWI in this region demonstrated a slight upward trend.

3.2. Joint probability constructions of wheat yields and drought indices

We calculated the Kendall's τ correlation between drought indices (SPI, SPAWI) and wheat yield across different periods. Table 3 presents the median correlation results from 27 GCM simulations for the grain filling stage at a 6-month scale, while results for other stages and scales are provided in Fig. S3.

In general, SPAWI exhibited closer correlations with yield than SPI except in WW. For example, the median correlation between SPAWI and yield in BA under all periods, SSPs, and CO_2 conditions was about 0.05 higher than that of SPI. Median correlations remained relatively consistent in different CO_2 conditions. For instance, the SPI-yield correlation was consistently measured around 0.5–0.6 in WA. Similarly, no significant differences were observed in median correlations under different SSP conditions. Overall, the correlations between the indices and wheat yield were moderate across all GCM simulations. We conducted validation tests for all drought index-wheat yield pairs, with the results detailed in Fig. S4. Subsequently, we constructed copulas using the pairs that passed all tests, and the results for the five candidate copula equations are shown in Table S5. We then used the joint probability functions to estimate wheat yield loss probabilities under drought conditions and to identify drought-trigger thresholds.

3.3. Variation of wheat yield loss probability and drought trigger thresholds

We used a copula function to calculate conditional probabilities of wheat yield loss under various drought conditions. Fig. 5 illustrates the median conditional probability based on 27 GCMs for the grain filling stage at a 6-month scale when SPI/SPAWI < -1. Across sites and periods, conditional yield loss probabilities based on SPAWI consistently exceeded those based on SPI, with the divergence enlarging toward the 2080s. CO_2 fertilization generally reduced probabilities for both indices, with larger relative reductions under SSP585 than SSP245. In WA, SPI-based probabilities remained moderate, whereas SPAWI was persistently higher, and CO_2 further suppressed probabilities, most noticeably

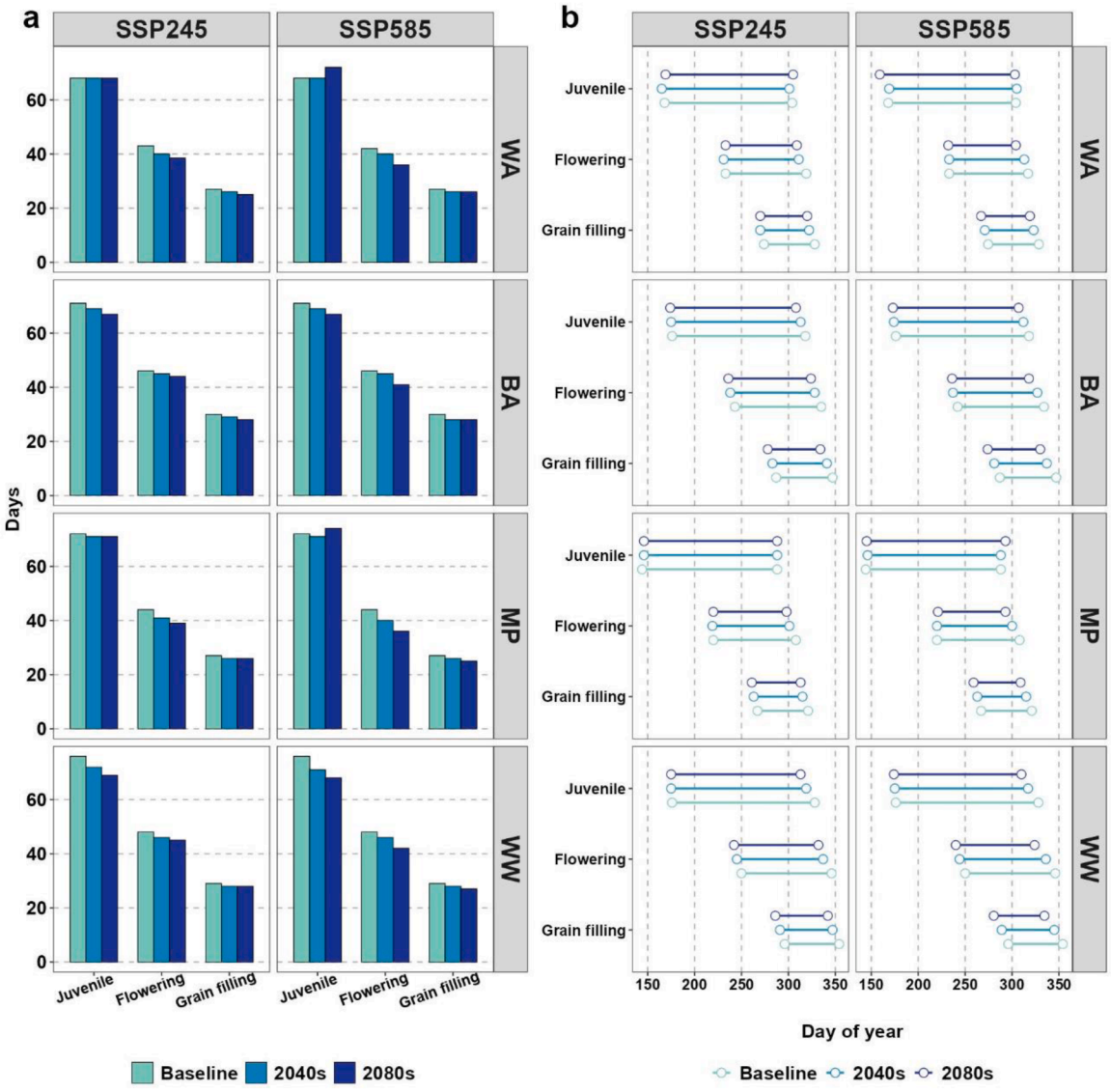

Fig. 3. Simulated duration and timing of wheat growth stages during the baseline period (1981–2020) and two future periods—the 2040s (2021–2060) and the 2080s (2061–2100) under SSP245 and SSP585 scenarios across four study sites. Values represent the median of projections from 27 GCMs used for each scenario.

for SPI in the 2080s. BA showed a steady rise in SPAWI through time with limited CO_2 sensitivity, and SPI remained lower. MP exhibited a progressive increase in SPAWI-based probabilities without CO_2 effects from the Baseline to the 2080s, reaching nearly 90%, with only modest CO_2 mitigation. In WW, probabilities were lower, but SPAWI still exceeded SPI, particularly by the 2080s. Moreover, CO_2 effects were more pronounced at all sites. In WA, CO_2 induced a gradual decline in both indices, especially SPI in the 2080s. BA recorded sharp CO_2-related decreases for both indices, though SPAWI remained higher than SPI. In MP, CO_2 markedly reduced SPAWI-based probabilities from about 90% without CO_2 to lower than 60% by the 2080s. WW also showed clear CO_2-driven reductions, with SPI decreasing substantially, and SPAWI likewise declined when CO_2 was included. Overall, SPAWI indicates a higher drought-related wheat yield loss probability than SPI, especially in MP and BA, and this gap widens over time. Nonetheless, CO_2 tends to moderate risks, most strongly under SSP585.

We identified drought index trigger thresholds (*DT*) for yield loss using the methodology described in Section 2.5. Therefore, the thresholds correspond to a 50% conditional probability and a conditional yield loss value equal to the 30th percentile of the average baseline yield. Here we present the results for the grain filling stage at a 6-month scale (Fig. 6), while results for other stages and scales are shown in Fig. S5. Thresholds closer to 0 indicate that milder droughts can cause heavy yield losses. At the baseline, SPI and SPAWI thresholds are closely aligned within sites (differences < 0.2) but vary markedly among sites, with drier western/northern locations requiring less negative thresholds than wetter eastern/southern sites. Under future climates, SPAWI thresholds generally exceed SPI, and CO_2 fertilization tends to lower thresholds, especially by the 2080s and under SSP585. In scenarios without CO_2, thresholds for both indices rise relative to the baseline, with larger increases under SSP585 and in the 2080s. For example, in BA under SSP245, median values of SPI/SPAWI shift from −0.28/−0.27 (2040s) to −0.25/−0.17 (2080s). However, in scenarios with CO_2 considered, thresholds decline relative to the baseline, with stronger declines under SSP585 and in the 2080s. For instance, in MP, median values of SPI/SPAWI change from −0.37/−0.41 (2040s) to −0.84/−0.72 (2080s). In general, the drought-triggering thresholds were higher at drier sites (WA, MP, BA) compared to the wetter site (WW).

We used ANOVA to analyze the factors contributing to the variation of drought-trigger thresholds (*DT*) for yield loss. Fig. 7 shows the results for the 6-month scale during the grain filling stage, with SPI shown in the inner rings and SPAWI in the outer rings, while results for other

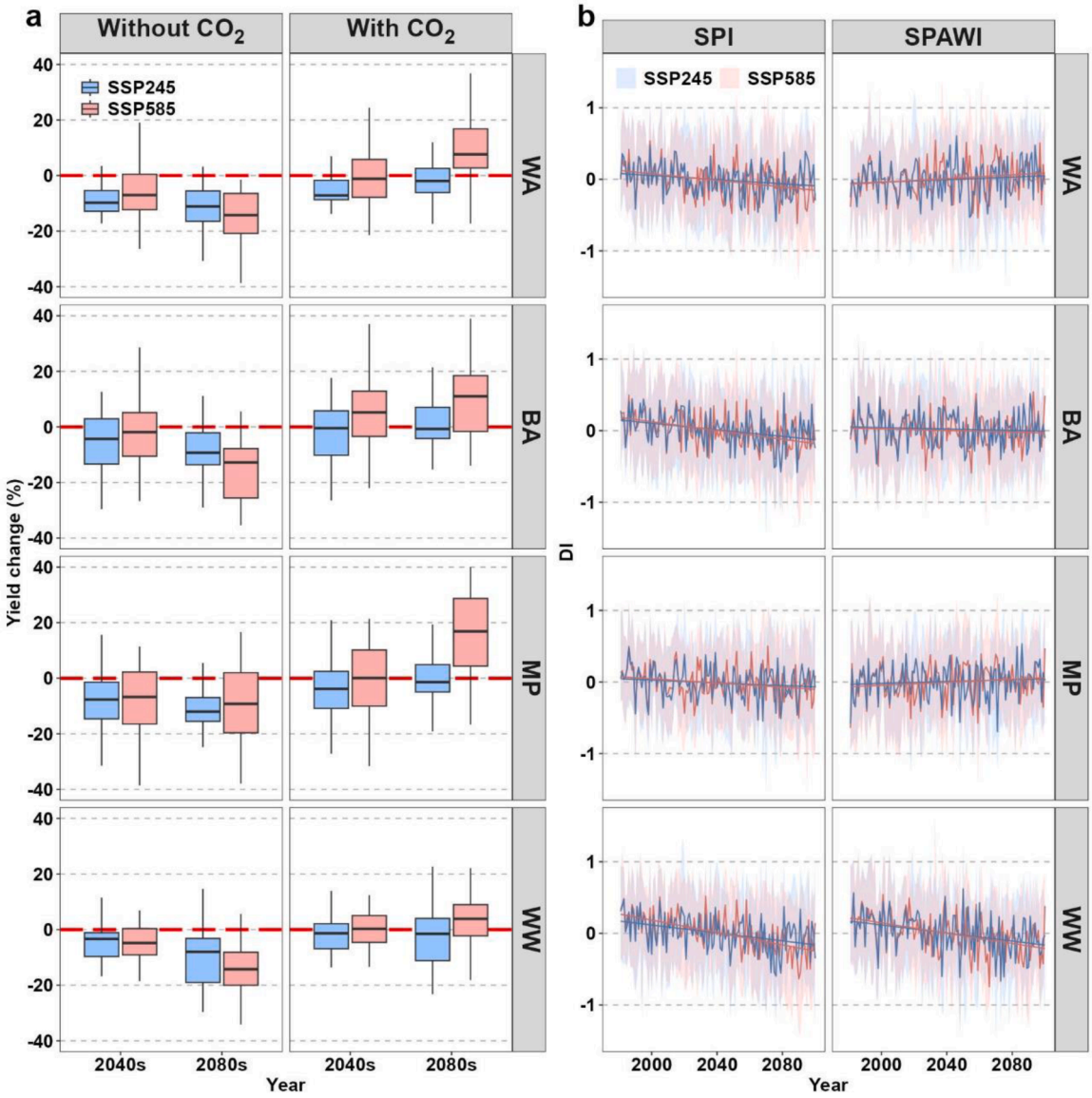

Fig. 4. Projected changes in wheat yield with and without CO_2 fertilization effects for two future periods (2040s and 2080s) under SSP245 and SSP585, along with time-series drought indices (SPI and SPAWI at a 6-month scale during the grain filling stage) from 2021 to 2100 at four study sites. For wheat yield, boxplot boundaries indicate the 25th and 75th percentiles, whiskers represent the 10th and 90th percentiles, and black lines within the boxes denote the median values across 27 GCMs. For drought indices, shaded areas indicate the interquartile range (25th–75th percentiles), and solid lines represent the GCM median and the linear trend over time.

scales and stages are provided in Fig. S6. Across sites and indices, GCM choice is the dominant source of *DT* variability, accounting for 51.1% to 66.7% of the total variance across all sites and drought indices. In contrast, the choice of emission scenarios (SSPs) alone was a negligible contributor, while CO_2 and GCM × SSP interactions exhibited varying impacts based on both the location and the drought index. These interactive effects were consistently more pronounced for SPAWI than for SPI. For instance, the GCM × SSP interaction explained 20.6% of the variance for SPAWI in WA, compared to only 13.2% for SPI. A similar pattern was observed in MP. Overall, GCM-related uncertainty dominates *DT* changes, with smaller, context-specific contributions from CO_2 and interactions.

4. Discussion

Using the APSIM crop model, we simulated future wheat growth in the NSW wheat belt under different SSP scenarios. Our results indicate a consistent trend of shortening and advancement of key growth stages (juvenile, flowering, and grain filling) in the future (Fig. 3). This phenological shift is primarily driven by rising temperatures, which accelerate thermal time accumulation and hasten wheat development (Li et al., 2022a; Sun et al., 2024; Ye et al., 2020). Our yield projections reveal a critical dependence on the CO_2 fertilization effect. When elevated CO_2 is considered, wheat yield shows an overall increase relative to the baseline, with greater gains under SSP585 than SSP245 and in the 2080s than in the 2040s (Fig. 4), consistent with previous studies (Azameti and Padaria, 2024; Orlov et al., 2024; Wen et al., 2023). This benefit stems from improved photosynthesis and water-use efficiency (Fan et al., 2023; Leakey et al., 2009). In contrast, simulations under constant CO_2 conditions exhibit a declining trend (Fig. 4), highlighting the adverse impacts of rising temperatures and altered rainfall, and thus underscoring the significant role of CO_2 in mitigating future climate-related yield losses.

Drought manifestations under future climate conditions exhibited distinct regional and index-specific patterns. Meteorological drought (SPI) is projected to intensify in southern sites, reflecting regional

Table 3
The median Kendall's τ correlation coefficients between wheat yield and drought indices (SPI, SPAWI) during the grain filling stage across 27 GCMs in the study regions. All results were statistically significant at the $p < 0.05$ level.

Site	Period	SSP	CO_2 effects	SPI	SPAWI
WA	2040s	SSP245	Without	0.546	0.594
			With	0.554	0.592
		SSP585	Without	0.544	0.582
			With	0.57	0.584
	2080s	SSP245	Without	0.528	0.561
			With	0.525	0.57
		SSP585	Without	0.504	0.567
			With	0.553	0.572
BA	2040s	SSP245	Without	0.616	0.669
			With	0.622	0.671
		SSP585	Without	0.585	0.649
			With	0.59	0.638
	2080s	SSP245	Without	0.641	0.659
			With	0.642	0.659
		SSP585	Without	0.564	0.649
			With	0.577	0.627
MP	2040s	SSP245	Without	0.55	0.61
			With	0.548	0.603
		SSP585	Without	0.541	0.601
			With	0.544	0.6
	2080s	SSP245	Without	0.562	0.588
			With	0.56	0.581
		SSP585	Without	0.596	0.563
			With	0.592	0.551
WW	2040s	SSP245	Without	0.702	0.617
			With	0.708	0.61
		SSP585	Without	0.695	0.585
			With	0.706	0.577
	2080s	SSP245	Without	0.716	0.636
			With	0.719	0.617
		SSP585	Without	0.681	0.61
			With	0.703	0.587

rainfall variability (Sahbeni et al., 2023; Samantaray et al., 2022; Tefera et al., 2024), while northern sites show little change (Fig. 4). Notably, the fitted trend lines suggest a less pronounced intensification of agricultural drought (SPAWI) compared to meteorological drought (Feng et al., 2024; Guo et al., 2025) (Fig. 4). This divergence can be attributed to the buffering capacity of soil, thereby mitigating crop water stress during low rainfall periods (He and Wang, 2019; Wang et al., 2019). Furthermore, meteorological indices like SPI can be misleading, as high rainfall may be lost to runoff or evaporation without benefiting the plant (Bennie and Hensley, 2001; Bodner et al., 2015). Our findings demonstrate that different drought indices capture varying aspects of crop water stress, emphasizing the necessity of using multiple indicators for an accurate agricultural drought assessment.

Additionally, our results show that yield loss probability varies with drought severity (Fig. 5), and these findings are consistent with previous research (Yang et al., 2024). However, the results also show differences in the probability range of yield loss under different drought indices. Specifically, for the same index value, SPAWI indicates a higher yield loss probability than SPI. This difference likely arises because changes in soil water content have a more direct and greater impact on crop yield than changes in rainfall (Zeleke, 2021). Boas et al. (2024) found that in areas with high soil water content, crop growth is not significantly affected by low rainfall because the stored soil water can mitigate drought-induced water stress, while lower soil water content will directly affect crop uptake and ultimately affect crop yield. Our findings support this view, demonstrating that the SPI, which incorporates rainfall, may potentially underestimate the probability of wheat yield loss compared with soil water-based SPAWI. Moreover, the projections indicate that the northeastern (MP) and southwestern (BA) sites will likely face more severe drought impacts in the future, highlighting these areas as priority targets for adaptation measures.

We further analyzed variations in *DT* for wheat yield loss with different drought indices and time periods. The results reveal clear regional differences in these thresholds (Fig. 6). The threshold change shows the regional variability of wheat yields caused by different rainfall and soil water content. During the baseline period, the 3-month SPI, being more sensitive to short-term deficits, often showed a higher (less negative) threshold than the 6-month SPI, particularly at the grain filling stage in southern sites like WW (Fig. S5). In contrast, under future climates, the 6-month thresholds became systematically higher than the 3-month thresholds, and this difference widened in the 2080s. Future variations in rainfall and soil water content contribute to different drought intensities across regions, ultimately affecting wheat growth and yield (Helman and Bonfil, 2022; Slater et al., 2022). Notably, SPAWI thresholds are consistently higher than those of SPI under projected future conditions, suggesting that agricultural drought, resulting from soil water stress, is more likely to induce wheat yield loss than meteorological drought caused by rainfall shortage. Furthermore, the progression of growth stages exerted a strong influence. In the baseline period, thresholds generally increased (became less negative) from juvenile to grain filling stages. However, this trend reversed under future projections, with thresholds decreasing at later stages, and the decline was more pronounced in the 2080s (Fig. S5). We also found that, in contrast to other sites, certain value thresholds in WW demonstrated higher median SPI thresholds compared to SPAWI. This may be attributed to the relatively wetter conditions in WW (Wang et al., 2018; Xiang et al., 2025), where superior soil water retention provides an effective buffering capacity that mitigates losses risk of drought-induced wheat yield (He et al., 2022). Consequently, soil water stress can more sensitively cause equivalent reductions in wheat yield than rainfall deficit. Furthermore, drought thresholds in the far future are lower than those in the near future. The impact is further amplified by higher CO_2 emission scenarios, as elevated CO_2 conditions under the SSP585 result in stronger fertilization effects and lower yield reduction compared to SSP245 (Orlov et al., 2024).

The contribution analysis of the future trigger threshold variation indicates that under different drought indices, changes in drought trigger thresholds are primarily driven by GCMs (Fig. 7). The differences observed might be attributed to varying rainfall simulations among climate models (Huang et al., 2022; Li et al., 2025a). Additionally, CO_2 concentrations also influence threshold changes at some sites. Increased CO_2 is known to reduce crop stomatal conductance, decrease transpiration, enhance water-use efficiency, and improve drought resistance, ultimately leading to higher crop yields (Sun et al., 2023; Wei et al., 2023a). Our findings confirm the yield-enhancing "CO_2 fertilization" effect, which is more pronounced under the high-emission SSP585 scenario than SSP245. This is also consistent with previous studies. For example, Wang et al. (2020) found an increasing change in wheat yield projection under increased CO_2 conditions in different climatic regions, especially under SSP585 scenarios in the far future. This effect also further influences the probability of wheat yield loss and the drought index threshold, since without the fertilizer effect of CO_2, wheat yields are more sensitive to drought under future climate change conditions, resulting in a higher probability of yield loss and higher *DT* values. Critically, this pattern of GCMs being the dominant source of uncertainty, followed by CO_2 effects, holds across different growth stages and time scales (Fig. S6). While the specific percentage contributions of each factor vary, there are no fundamental shifts in their relative importance.

Our multi-site explicit analysis of drought thresholds offers several actionable pathways for enhancing climate resilience for drought-prone regions, such as in the NSW wheat belt. For agricultural practitioners, the divergence between SPI and SPAWI thresholds underscores the necessity of moving beyond rainfall-based drought monitoring. Farmers, particularly in high-risk regions, should adopt soil moisture-based decision support systems, using our identified SPAWI threshold as early-warning triggers for implementing drought management strategies during critical growth stages. Furthermore, the projected lowering of thresholds in certain areas under future climates signals an urgent need

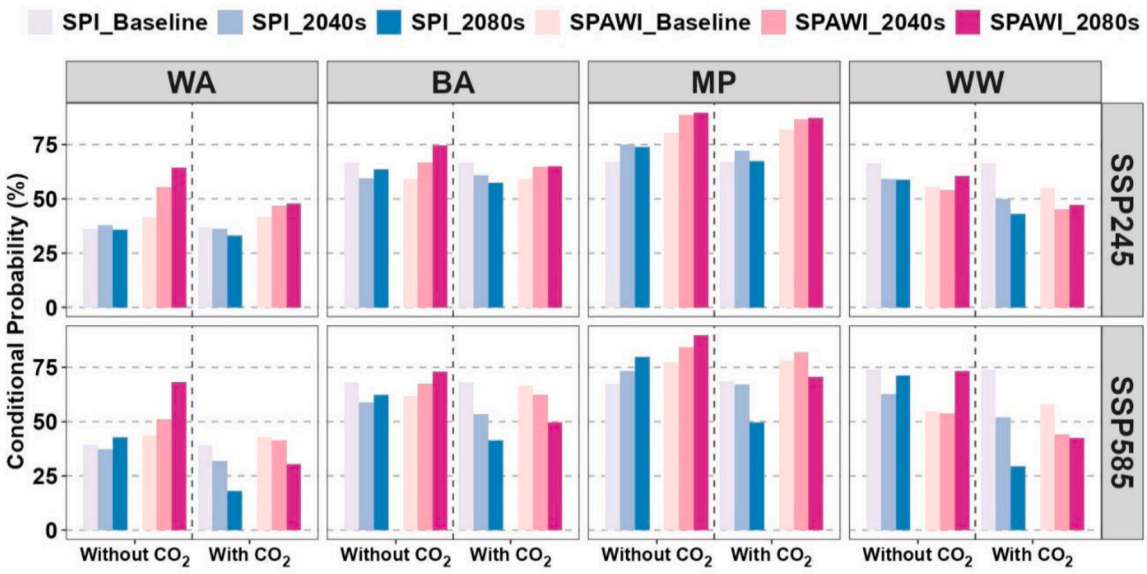

Fig. 5. Projected conditional probability of yield loss under drought conditions (SPI/SPAWI < -1) in the 2040s and 2080s under the SSP245 and SSP585 at four study sites. The bar values represent the median conditional probability of 27 GCMs that passed the tests.

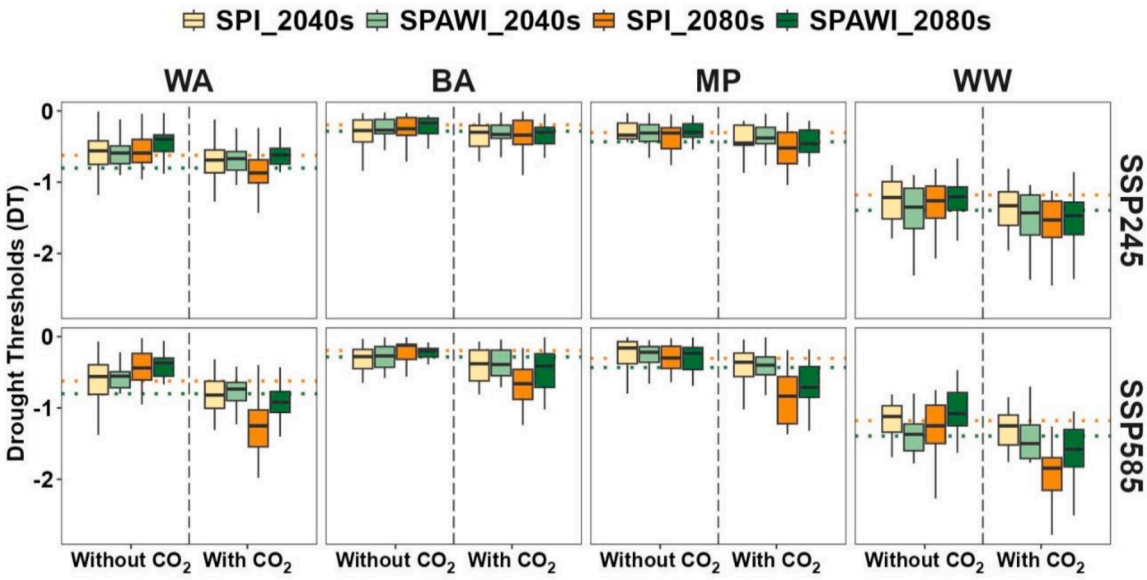

Fig. 6. Projected drought thresholds (*DT*) in the 2040s and 2080s under SSP245 and SSP585 scenarios at four study sites. The boundaries of the box represent the 25th and 75th percentiles among 27 GCMs that passed the tests, while the whiskers below and above the box depict the 5th and 95th percentiles. Within each box, the black line shows the multi-model median. The orange and green dashed lines represent the thresholds of SPI and SPAWI for the baseline period, respectively.

for long-term adaptation through the adoption of more drought-resilient crop varieties. Our findings also provide a scientific basis for policy-makers to allocate resources effectively. Investment in climate adaptation infrastructure, such as subsidies for soil moisture probes, should be prioritized in the vulnerable western sub-regions. Moreover, the quantified thresholds can serve as transparent and objective triggers for regionalized index-based insurance schemes, ensuring timely financial support to affected farmers while minimizing administrative costs. Finally, integrating these sub-regional thresholds into the state's agricultural extension services would enable a more precise and effective early-warning system, ultimately safeguarding Australia's food security in a changing climate.

Nonetheless, there are several limitations to our study. A key consideration is our reliance on a single crop model. While APSIM has been widely validated for wheat in Australia and provides a mechanistically consistent framework (Anwar et al., 2024; Chen et al., 2023; Tan et al., 2025), our findings are inherently influenced by its specific representations of soil hydrological processes and crop physiology (Ruane et al., 2021; Zheng and Zhang, 2025). Consequently, the use of a single model has limited our ability to quantify of structural uncertainty inherent in crop modelling (Wang et al., 2024a). Comparative studies, like those undertaken by the Agricultural Model Intercomparison and Improvement Project (AgMIP) (Rosenzweig et al., 2013), have shown that different models can produce a range of projections for drought impact due to variations in their core algorithms (Durand et al., 2018; Kimball et al., 2019; Sweet et al., 2025). Therefore, our results should be interpreted as a plausible trajectory within a broader spectrum of possible outcomes. Future research would benefit from employing a

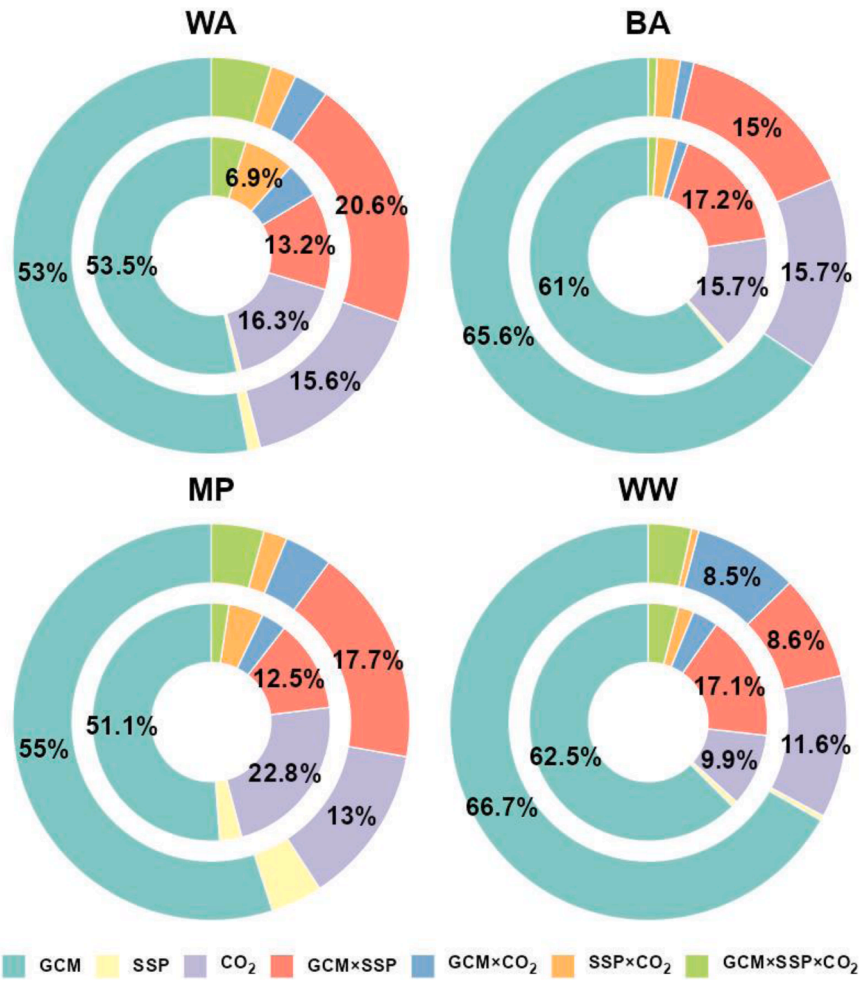

Fig. 7. The different sources (GCMs, SSP scenarios, and CO_2 effects) of contribution to the identified drought threshold at four study sites. The inner circle shows the contribution of each source to SPI, while the outer circle illustrates the contribution to SPAWI.

multi-model ensemble to better constrain this uncertainty and enhance the robustness of risk assessments. Moreover, the projected mitigating effect of elevated CO_2 on yield loss carries significant uncertainty (Rezaei et al., 2023). While represented in APSIM according to current understanding, the realized CO_2 fertilization effect in farmers' fields may be constrained by other factors, such as nitrogen limitation or ozone damage (Leung et al., 2022; Terrer et al., 2019). Consequently, our results that include CO_2 effects may represent a more optimistic scenario, and the risks under drought conditions could be even higher. In addition, our analysis focused on drought as a primary stressor. We did not account for the effects of compound extreme events, such as heatwaves coinciding with drought, which are projected to increase in frequency and can have devastating, non-linear impacts on crop yields (Li et al., 2025b). Incorporating compound hazard metrics and heat-damage functions within the crop model would likely sharpen risk estimates.

5. Conclusion

We assessed wheat yield loss risk and the change of drought-trigger thresholds with and without the impact of CO_2 fertilization using a process-based crop model and the copula method. Our analysis demonstrates that future wheat yield loss risk is best captured by the agricultural drought index (SPAWI), which shows higher risk and thresholds than the meteorological index (SPI). While CO_2 fertilization moderates risk by lowering drought thresholds, this effect is subject to significant climate model uncertainty. The spatial variation in thresholds underscores the need for region-specific adaptation strategies. Therefore, moving beyond meteorological indices to monitor soil water is essential for accurate risk assessment and developing targeted interventions to safeguard wheat production under climate change.

CRediT authorship contribution statement

Keyu Xiang: Writing – review & editing, Writing – original draft, Validation, Software, Methodology, Data curation, Conceptualization. **Bin Wang:** Writing – review & editing, Software, Methodology, Conceptualization. **De Li Liu:** Writing – review & editing, Software, Methodology, Data curation. **Chao Chen:** Writing – review & editing, Methodology. **Fei Ji:** Writing – review & editing, Methodology. **Fangzheng Chen:** Software, Methodology. **Shijin Yao:** Validation, Software, Methodology. **Siyi Li:** Software, Data curation. **Alfredo Huete:** Writing – review & editing, Supervision. **Yi Li:** Methodology. **Qiang Yu:** Writing – review & editing, Supervision, Resources.

Declaration of competing interest

The authors declare that they have no known competing financial interests or personal relationships that could have appeared to influence the work reported in this paper.

Acknowledgement

The first author acknowledges the China Scholarship Council for the financial support of his PhD study (No.202006300006). Facilities for

conducting this study were provided by the New South Wales Department of Primary Industries and University of Technology Sydney. Thanks to Grains Research and Development Corporation National Variety Trials, Australia (GRDC-NVT) (https://nvt.grdc.com.au//) and Soil Moisture Integration and Prediction System (SMIPS) (https://dx.doi.org/10.25901/b020-nm39) for the data support. We are grateful to the editor and two anonymous reviewers for their constructive feedback and comments, which have helped to improve the manuscript.

Supplementary materials

Supplementary material associated with this article can be found, in the online version, at doi:10.1016/j.agrformet.2025.111003.

Data availability

Data will be made available on request.

References

Aghakouchak, A., Hao, Z., 2014. A nonparametric multivariate multi-index drought monitoring framework. J. Hydrometeorol. 15, 89–101. https://doi.org/10.1175/jhm-d-12-0160.1.

Ahuja, L.R., Anapalli, S., Feng, G., Feng, P., Flerchinger, G.N., Green, T.R., Hoogenboom, G., Hu, K., Irmak, S., Kersebaum, K.C., Kukal, M.S., Liu, D.L., Lizaso, J. I., Perrier, A., Seyfried, M.S., Shaffer, M.J., Shelia, V., Skaggs, T.H., Stöckle, C.O., Suarez, D.L., Timlin, D.J., Tuzet, A.J., Wang, B., Don Wauchope, R., Wendroth, O., Yu, Q., 2022. Modeling Processes and Their Interactions in Cropping Systems Challenges for the 21st Century. John Wiley & Sons, India.

Angelidis, P., Maris, F., Kotsovinos, N., Hrissanthou, V., 2012. Computation of drought index SPI with alternative distribution functions. Water Resour. Manag. 26, 2453–2473. https://doi.org/10.1007/s11269-012-0026-0.

Anwar, M.R., Emebiri, L., Ip, R.H.L., Luckett, D.J., Chauhan, Y.S., Zeleke, K.T., 2024. Least absolute shrinkage and selection operator regression used to select important features when predicting wheat yield from various genotype groups. J. Agric. Sci. 162, 245–259. https://doi.org/10.1017/s0021859624000479.

Asseng, S., Ewert, F., Martre, P., Rötter, R.P., Lobell, D.B., Cammarano, D., Kimball, B.A., Ottman, M.J., Wall, G.W., White, J.W., Reynolds, M.P., Alderman, P.D., Prasad, P.V. V., Aggarwal, P.K., Anothai, J., Basso, B., Biernath, C., Challinor, A.J., De Sanctis, G., Doltra, J., Fereres, E., Garcia-Vila, M., Gayler, S., Hoogenboom, G., Hunt, L.A., Izaurralde, R.C., Jabloun, M., Jones, C.D., Kersebaum, K.C., Koehler, A.K., Müller, C., Naresh Kumar, S., Nendel, C., O'leary, G., Olesen, J.E., Palosuo, T., Priesack, E., Eyshi Rezaei, E., Ruane, A.C., Semenov, M.A., Shcherbak, I., Stöckle, C., Stratonovitch, P., Streck, T., Supit, I., Tao, F., Thorburn, P.J., Waha, K., Wang, E., Wallach, D., Wolf, J., Zhao, Z., Zhu, Y., 2014. Rising temperatures reduce global wheat production. Nat. Clim. Chang. 5, 143–147. https://doi.org/10.1038/nclimate2470.

Asseng, S., Martre, P., Maiorano, A., Rotter, R.P., O'leary, G.J., Fitzgerald, G.J., Girousse, C., Motzo, R., Giunta, F., Babar, M.A., Reynolds, M.P., Kheir, A.M.S., Thorburn, P.J., Waha, K., Ruane, A.C., Aggarwal, P.K., Ahmed, M., Balkovic, J., Basso, B., Biernath, C., Bindi, M., Cammarano, D., Challinor, A.J., De Sanctis, G., Dumont, B., Eyshi Rezaei, E., Fereres, E., Ferrise, R., Garcia-Vila, M., Gayler, S., Gao, Y., Horan, H., Hoogenboom, G., Izaurralde, R.C., Jabloun, M., Jones, C.D., Kassie, B.T., Kersebaum, K.C., Klein, C., Koehler, A.K., Liu, B., Minoli, S., Montesino San Martin, M., Muller, C., Naresh Kumar, S., Nendel, C., Olesen, J.E., Palosuo, T., Porter, J.R., Priesack, E., Ripoche, D., Semenov, M.A., Stockle, C., Stratonovitch, P., Streck, T., Supit, I., Tao, F., Van Der Velde, M., Wallach, D., Wang, E., Webber, H., Wolf, J., Xiao, L., Zhang, Z., Zhao, Z., Zhu, Y., Ewert, F., 2019. Climate change impact and adaptation for wheat protein. Glob. Chang. Biol. 25, 155–173. https://doi.org/10.1111/gcb.14481.

Azameti, M.K., Padaria, J.C., 2024. Understanding wheat thermo-tolerance mechanisms for enhanced sustainable production. In: Sheraz Mahdi, S., Singh, R., Dhekale, B. (Eds.), Adapting to Climate Change in Agriculture-Theories and Practices: Approaches for Adapting to Climate Change in Agriculture in India. Springer Cham, Cham, pp. 143–161.

Barua, S., Ng, A.W.M., Perera, B.J.C., 2011. Comparative evaluation of drought indexes: case study on the Yarra River catchment in Australia. J. Water Resour. Plan. Manag. 137, 215–226. https://doi.org/10.1061/(asce)wr.1943-5452.0000105.

Bennie, A.T.P., Hensley, M., 2001. Maximizing precipitation utilization in dryland agriculture in South Africa–a review. J. Hydrol. 241, 124–139. https://doi.org/10.1016/S0022-1694(00)00377-2.

Boas, T., Bogena, H., Ryu, D., Western, A., Hendricks Franssen, H.J., 2024. Multi-decadal soil moisture and crop yield variability–a case study with the community land model (CLM5). J. Adv. Model. Earth Syst. 16. https://doi.org/10.1029/2023ms004023 e2023MS004023.

Bodner, G., Nakhforoosh, A., Kaul, H.P., 2015. Management of crop water under drought: a review. Agron. Sustain. Dev. 35, 401–442. https://doi.org/10.1007/s13593-015-0283-4.

Boeing, F., Rakovec, O., Kumar, R., Samaniego, L., Schrön, M., Hildebrandt, A., Rebmann, C., Thober, S., Müller, S., Zacharias, S., Bogena, H., Schneider, K., Kiese, R., Attinger, S., Marx, A., 2022. High-resolution drought simulations and comparison to soil moisture observations in Germany. Hydrol. Earth Syst. Sci. 26, 5137–5161. https://doi.org/10.5194/hess-26-5137-2022.

Chen, C., Ota, N., Wang, B., Fu, G., Fletcher, A., 2023. Adaptation to climate change through strategic integration of long fallow into cropping system in a dryland Mediterranean-type environment. Sci. Total Environ. 880, 163230. https://doi.org/10.1016/j.scitotenv.2023.163230.

Chen, F., Xu, X., Chen, S., Wang, Z., Wang, B., Zhang, Y., Zhang, C., Feng, P., Hu, K., 2024. Soil buffering capacity enhances maize yield resilience amidst climate perturbations. Agric. Syst. 215, 103870. https://doi.org/10.1016/j.agsy.2024.103870.

Chen, X., Li, Y., Yao, N., Liu, D.L., Javed, T., Liu, C., Liu, F., 2020. Impacts of multi-timescale SPEI and SMDI variations on winter wheat yields. Agric. Syst. 185, 102955. https://doi.org/10.1016/j.agsy.2020.102955.

Clarke, D., Hess, T.M., Haro-Monteagudo, D., Semenov, M.A., Knox, J.W., 2021. Assessing future drought risks and wheat yield losses in England. Agric. For. Meteorol. 297, 108248. https://doi.org/10.1016/j.agrformet.2020.108248.

Devanand, A., Falster, M.G., Gillett, E.Z., Hobeichi, S., Holgate, M.C., Jin, C., Mu, M., Parker, T., Rifai, W.S., Rome, S.K., Stojanovic, M., Vogel, E., Abram, J.N., Abramowitz, G., Coats, S., Evans, P.J., Gallant, J.E.A., Pitman, J.A., Power, B.S., Rauniyar, P.S., Taschetto, S.A., Ukkola, M.A., 2024. Australia's Tinderbox drought an extreme natural event likely worsened by human-caused climate change. Sci. Adv. 10, eadj3460. https://doi.org/10.1126/sciadv.adj3460.

Dreccer, M.F., Fainges, J., Whish, J., Ogbonnaya, F.C., Sadras, V.O., 2018. Comparison of sensitive stages of wheat, barley, canola, chickpea and field pea to temperature and water stress across Australia. Agric. For. Meteorol. 248, 275–294. https://doi.org/10.1016/j.agrformet.2017.10.006.

Dubois, E., Larocque, M., 2024. Contribution of standardized indexes to understand groundwater level fluctuations in response to meteorological conditions in cold and humid climates. J. Hydrol. 634, 131105. https://doi.org/10.1016/j.jhydrol.2024.131105.

Durand, J.L., Delusca, K., Boote, K., Lizaso, J., Manderscheid, R., Weigel, H.J., Ruane, A. C., Rosenzweig, C., Jones, J., Ahuja, L., Anapalli, S., Basso, B., Baron, C., Bertuzzi, P., Biernath, C., Deryng, D., Ewert, F., Gaiser, T., Gayler, S., Heinlein, F., Kersebaum, K. C., Kim, S.H., Müller, C., Nendel, C., Olioso, A., Priesack, E., Villegas, J.R., Ripoche, D., Rötter, R.P., Seidel, S.I., Srivastava, A., Tao, F., Timlin, D., Twine, T., Wang, E., Webber, H., Zhao, Z., 2018. How accurately do maize crop models simulate the interactions of atmospheric CO2 concentration levels with limited water supply on water use and yield? Eur. J. Agron. 100, 67–75. https://doi.org/10.1016/j.eja.2017.01.002.

Fan, J., Wu, X., Yu, Y., Zuo, Q., Shi, J., Halpern, M., Sheng, J., Jiang, P., Ben-Gal, A., 2023. Characterizing root-water-uptake of wheat under elevated CO2 concentration. Agric. Water Manag. 275, 108005. https://doi.org/10.1016/j.agwat.2022.108005.

Farahmand, A., Aghakouchak, A., 2015. A generalized framework for deriving nonparametric standardized drought indicators. Adv. Water Resour. 76, 140–145. https://doi.org/10.1016/j.advwatres.2014.11.012.

Feldman, A.F., Konings, A.G., Gentine, P., Cattry, M., Wang, L., Smith, W.K., Biederman, J.A., Chatterjee, A., Joiner, J., Poulter, B., 2024. Large global-scale vegetation sensitivity to daily rainfall variability. Nature 636, 380–384. https://doi.org/10.1038/s41586-024-08232-z.

Feng, K., Wang, Y., Li, Y., Wang, F., Su, X., Zhang, Z., Wu, H., Zhang, G., Li, Y., Wang, X., 2024. Three-dimensional perspective on the characterization of the spatiotemporal propagation from meteorological to agricultural drought. Agric. For. Meteorol. 353, 110048. https://doi.org/10.1016/j.agrformet.2024.110048.

Feng, P., Wang, B., Liu, D.L., Waters, C., Xiao, D., Shi, L., Yu, Q., 2020a. Dynamic wheat yield forecasts are improved by a hybrid approach using a biophysical model and machine learning technique. Agric. For. Meteorol. 285–286. https://doi.org/10.1016/j.agrformet.2020.107922.

Feng, P., Wang, B., Liu, D.L., Waters, C., Yu, Q., 2019. Incorporating machine learning with biophysical model can improve the evaluation of climate extremes impacts on wheat yield in south-eastern Australia. Agric. For. Meteorol. 275, 100–113. https://doi.org/10.1016/j.agrformet.2019.05.018.

Feng, P., Wang, B., Luo, J.J., Liu, L., Waters, C., Ji, F., Ruan, H., Xiao, D., Shi, L., Yu, Q., 2020b. Using large-scale climate drivers to forecast meteorological drought condition in growing season across the Australian wheatbelt. Sci. Total Environ. 724, 138162. https://doi.org/10.1016/j.scitotenv.2020.138162.

Feng, P., Wang, B., Macadam, I., Taschetto, A.S., Abram, N.J., Luo, J.J., King, A.D., Chen, Y., Li, Y., Liu, L., Yu, Q., Hu, K., 2022. Increasing dominance of Indian Ocean variability impacts Australian wheat yields. Nat. Food 3, 862–870. https://doi.org/10.1038/s43016-022-00613-9.

Gajurel, S., Lai, Y., Lobsey, C., Pembleton, K.G., 2024. A cost-effective approach to estimate plant available water capacity. Geoderma 442, 116794. https://doi.org/10.1016/j.geoderma.2024.116794.

Gebrechorkos, S.H., Sheffield, J., Vicente-Serrano, S.M., Funk, C., Miralles, D.G., Peng, J., Dyer, E., Talib, J., Beck, H.E., Singer, M.B., Dadson, S.J., 2025. Warming accelerates global drought severity. Nature 642, 628–635. https://doi.org/10.1038/s41586-025-09047-2.

Genest, C., Favre, A.C., 2007. Everything you always wanted to know about copula modeling but were afraid to ask. J. Hydrol. Eng. 12, 347–368. https://doi.org/10.1061/(ASCE)1084-0699(2007)12:4(347).

Geruo, A., Zhao, M., Velicogna, I., Kimball, J.S., 2017. A global gridded dataset of GRACE drought Severity Index for 2002–14: comparison with PDSI and SPEI and a case study of the Australia millennium drought. J. Hydrometeorol. 18, 2117–2129. https://doi.org/10.1175/jhm-d-16-0182.1.

Gringorten, I.I., 1963. A plotting rule for extreme probability paper. J. Geophys. Res. 68, 813–814. https://doi.org/10.1029/JZ068i003p00813.

Gunar, S., Trenkler, D., 1995. Exact and randomization distributions of Kolmogorov-Smirnov tests two or three samples. Comput. Stat. Data Anal. 20, 185–202. https://doi.org/10.1016/0167-9473(94)00040-P.

Guo, L., Chen, F., Wang, B., Liu, D.L., Chen, X., Huang, H., Bai, H., Liao, K., Xia, Z., Xiang, K., Li, L., Zheng, T., Yu, Q., 2025. Developing a multivariate drought index to assess drought characteristics based on the SWAT-Copula method in the Poyang Lake basin, China. Ecol. Indic. 170, 113123. https://doi.org/10.1016/j.ecolind.2025.113123.

Guo, W., Huang, S., Huang, Q., Leng, G., Mu, Z., Han, Z., Wei, X., She, D., Wang, H., Wang, Z., Peng, J., 2023. Drought trigger thresholds for different levels of vegetation loss in China and their dynamics. Agric. For. Meteorol. 331, 109349. https://doi.org/10.1016/j.agrformet.2023.109349.

Gupta, A., Rico-Medina, A., Caño-Delgado, I.A., 2020. The physiology of plant responses to drought. Science 368, 266–269. https://doi.org/10.1126/science.aaz7614.

Han, Z., Huang, S., Huang, Q., Leng, G., Liu, Y., Bai, Q., He, P., Liang, H., Shi, W., 2021. GRACE-based high-resolution propagation threshold from meteorological to groundwater drought. Agric. For. Meteorol. 307, 108476. https://doi.org/10.1016/j.agrformet.2021.108476.

Han, Z., Huang, S., Peng, J., Li, J., Leng, G., Huang, Q., Zhao, J., Yang, F., He, P., Meng, X., Li, Z., 2023. GRACE-based dynamic assessment of hydrological drought trigger thresholds induced by meteorological drought and possible driving mechanisms. Remote Sens. Environ. 298, 113831. https://doi.org/10.1016/j.rse.2023.113831.

Hao, Y., Yuan, X., Zhang, M., 2024. Enhanced relationship between seasonal soil moisture droughts and vegetation under climate change over China. Agric. For. Meteorol. 358, 110258. https://doi.org/10.1016/j.agrformet.2024.110258.

Hao, Z., Hao, F., Singh, V.P., Ouyang, W., 2017. Quantitative risk assessment of the effects of drought on extreme temperature in eastern China. J. Geophys. Res. Atmos. 122, 9050–9059. https://doi.org/10.1002/2017jd027030.

Hao, Z., Singh, V.P., 2015. Drought characterization from a multivariate perspective: a review. J. Hydrol. 527, 668–678. https://doi.org/10.1016/j.jhydrol.2015.05.031.

He, D., Oliver, Y., Rab, A., Fisher, P., Armstrong, R., Kitching, M., Wang, E., 2022. Plant available water capacity (PAWC) of soils predicted from crop yields better reflects within-field soil physicochemical variations. Geoderma 422, 115958. https://doi.org/10.1016/j.geoderma.2022.115958.

He, D., Wang, E., 2019. On the relation between soil water holding capacity and dryland crop productivity. Geoderma 353, 11–24. https://doi.org/10.1016/j.geoderma.2019.06.022.

Helman, D., Bonfil, D.J., 2022. Six decades of warming and drought in the world's top wheat-producing countries offset the benefits of rising CO(2) to yield. Sci. Rep. 12, 7921. https://doi.org/10.1038/s41598-022-11423-1.

Hendrawan, V.S.A., Kim, W., Touge, Y., Ke, S., Komori, D., 2022. A global-scale relationship between crop yield anomaly and multiscalar drought index based on multiple precipitation data. Environ. Res. Lett. 17, 014037. https://doi.org/10.1088/1748-9326/ac45b4.

Holzworth, D.P., Huth, N.I., Devoil, P.G., Zurcher, E.J., Herrmann, N.I., Mclean, G., Chenu, K., Van Oosterom, E.J., Snow, V., Murphy, C., Moore, A.D., Brown, H., Whish, J.P.M., Verrall, S., Fainges, J., Bell, L.W., Peake, A.S., Poulton, P.L., Hochman, Z., Thorburn, P.J., Gaydon, D.S., Dalgliesh, N.P., Rodriguez, D., Cox, H., Chapman, S., Doherty, A., Teixeira, E., Sharp, J., Cichota, R., Vogeler, I., Li, F.Y., Wang, E., Hammer, G.L., Robertson, M.J., Dimes, J.P., Whitbread, A.M., Hunt, J., Van Rees, H., Mcclelland, T., Carberry, P.S., Hargreaves, J.N.G., Macleod, N., Mcdonald, C., Harsdorf, J., Wedgwood, S., Keating, B.A., 2014. APSIM–evolution towards a new generation of agricultural systems simulation. Environ. Model. Softw. 62, 327–350. https://doi.org/10.1016/j.envsoft.2014.07.009.

Hosseinzadehtalaei, P., Termonia, P., Tabari, H., 2024. Projected changes in compound hot-dry events depend on the dry indicator considered. Commun. Earth Environ. 5, 220. https://doi.org/10.1038/s43247-024-01352-4.

Hou, M., Li, Y., Biswas, A., Chen, X., Xie, L., Liu, D., Li, L., Feng, H., Wu, S., Satoh, Y., Pulatov, A., Siddique, K.H.M., 2024. Concurrent drought threatens wheat and maize production and will widen crop yield gaps in the future. Agric. Syst. 220, 104056. https://doi.org/10.1016/j.agsy.2024.104056.

Huang, M., Wang, J., Wang, B., Liu, D.L., Feng, P., Yu, Q., Pan, X., Li, S., Jiang, T., 2022. Dominant sources of uncertainty in simulating maize adaptation under future climate scenarios in China. Agric. Syst. 199, 103411. https://doi.org/10.1016/j.agsy.2022.103411.

Huang, S., Wang, L., Wang, H., Huang, Q., Leng, G., Fang, W., Zhang, Y., 2019. Spatio-temporal characteristics of drought structure across China using an integrated drought index. Agric. Water Manag. 218, 182–192. https://doi.org/10.1016/j.agwat.2019.03.053.

Huang, W., Prokhorov, A., 2014. A goodness-of-fit test for copulas. Econom. Rev. 33, 751–771. https://doi.org/10.1080/07474938.2012.690692.

IPCC, 2021. Climate change 2021: the physical science basis. Contribution of Working Group I to the Sixth Assessment Report of the Intergovernmental Panel On Climate Change. IPCC. Cambridge, United Kingdom and New York, NY, USA.

Jeffrey, S.J., Carter, J.O., Moodie, K.B., Beswick, A.R., 2001. Using spatial interpolation to construct a comprehensive archive of Australian climate data. Environ. Model. Softw. 16, 309–330. https://doi.org/10.1016/S1364-8152(01)00008-1.

Kanthavel, P., Saxena, C.K., Singh, R.K., 2022. Integrated drought index based on vine copula modelling. Int. J. Climatol. 42, 9510–9529. https://doi.org/10.1002/joc.7840.

Keating, B.A., Carberry, P.S., Hammer, G.L., Probert, M.E., Robertson, M.J., Holzworth, D., Huth, N.I., Hargreaves, J.N.G., Meinke, H., Hochman, Z., Mclean, G., Verburg, K., Snow, V., Dimes, J.P., Silburn, M., Wang, E., Brown, S., Bristow, K.L., Asseng, S., Chapman, S., Mccown, R.L., Freebairn, D.M., Smith, C.J., 2003. An overview of APSIM, a model designed for farming systems simulation. Eur. J. Agron. 18, 267–288.

Kimball, B.A., Boote, K.J., Hatfield, J.L., Ahuja, L.R., Stockle, C., Archontoulis, S., Baron, C., Basso, B., Bertuzzi, P., Constantin, J., Deryng, D., Dumont, B., Durand, J. L., Ewert, F., Gaiser, T., Gayler, S., Hoffmann, M.P., Jiang, Q., Kim, S.H., Lizaso, J., Moulin, S., Nendel, C., Parker, P., Palosuo, T., Priesack, E., Qi, Z., Srivastava, A., Stella, T., Tao, F., Thorp, K.R., Timlin, D., Twine, T.E., Webber, H., Willaume, M., Williams, K., 2019. Simulation of maize evapotranspiration: an inter-comparison among 29 maize models. Agric. For. Meteorol. 271, 264–284. https://doi.org/10.1016/j.agrformet.2019.02.037.

King, A.D., Pitman, A.J., Henley, B.J., Ukkola, A.M., Brown, J.R., 2020. The role of climate variability in Australian drought. Nat. Clim. Chang. 10, 177–179. https://doi.org/10.1038/s41558-020-0718-z.

Kukal, M.S., Irmak, S., Dobos, R., Gupta, S., 2023. Atmospheric dryness impacts on crop yields are buffered in soils with higher available water capacity. Geoderma 429, 116270. https://doi.org/10.1016/j.geoderma.2022.116270.

Leakey, A.D., Ainsworth, E.A., Bernacchi, C.J., Rogers, A., Long, S.P., Ort, D.R., 2009. Elevated CO2 effects on plant carbon, nitrogen, and water relations: six important lessons from FACE. J. Exp. Bot. 60, 2859–2876. https://doi.org/10.1093/jxb/erp096.

Leung, F., Sitch, S., Tai, A.P.K., Wiltshire, A.J., Gornall, J.L., Folberth, G.A., Unger, N., 2022. CO2 fertilization of crops offsets yield losses due to future surface ozone damage and climate change. Environ. Res. Lett. 17, 074007. https://doi.org/10.1088/1748-9326/ac7246.

Li, J., Wang, Z., Wu, X., Zscheischler, J., Guo, S., Chen, X., 2021. A standardized index for assessing sub-monthly compound dry and hot conditions with application in China. Hydrol. Earth Syst. Sci. 25, 1587–1601. https://doi.org/10.5194/hess-25-1587-2021.

Li, L., He, Q., Harrison, M.T., Shi, Y., Feng, P., Wang, B., Zhang, Y., Li, Y., Liu, D.L., Yang, G., Zhou, M., Yu, Q., Liu, K., 2025a. Knowledge-guided machine learning for improving crop yield projections of waterlogging effects under climate change. Resour. Environ. Sustain. 19, 100185. https://doi.org/10.1016/j.resenv.2024.100185.

Li, L., Zhang, Y., Wang, B., Feng, P., He, Q., Shi, Y., Liu, K., Harrison, M.T., Liu, D.L., Yao, N., Li, Y., He, J., Feng, H., Siddique, K.H.M., Yu, Q., 2023. Integrating machine learning and environmental variables to constrain uncertainty in crop yield change projections under climate change. Eur. J. Agron. 149, 126917. https://doi.org/10.1016/j.eja.2023.126917.

Li, M., Tang, Y., Li, C., Wu, X., Tao, X., Liu, M., 2022a. Climate warming causes changes in wheat phenological development that benefit yield in the Sichuan Basin of China. Eur. J. Agron. 139, 126574. https://doi.org/10.1016/j.eja.2022.126574.

Li, P., Huang, Q., Huang, S., Leng, G., Peng, J., Wang, H., Zheng, X., Li, Y., Fang, W., 2022b. Various maize yield losses and their dynamics triggered by drought thresholds based on copula-bayesian conditional probabilities. Agric. Water Manag. 261, 107391. https://doi.org/10.1016/j.agwat.2021.107391.

Li, S., Wang, B., Feng, P., Liu, D.L., Li, L., Shi, L., Yu, Q., 2022c. Assessing climate vulnerability of historical wheat yield in south-eastern Australia's wheat belt. Agric. Syst. 196, 103340. https://doi.org/10.1016/j.agsy.2021.103340.

Li, S., Wang, B., Liu, D.L., Chen, C., Feng, P., Huang, M., Wang, X., Shi, L., Waters, C., Huete, A., Yu, Q., 2024. Can agronomic options alleviate the risk of compound drought-heat events during the wheat flowering period in southeastern Australia? Eur. J. Agron. 153, 127030. https://doi.org/10.1016/j.eja.2023.127030.

Li, S., Wang, B., Liu, D.L., Chen, C., Feng, P., Huete, A., Xiang, K., Yu, Q., 2025b. The contribution of climate drivers to compound drought and extreme temperature events increased in recent decades. Weather Clim. Extrem. 49, 100793. https://doi.org/10.1016/j.wace.2025.100793.

Liu, D.L., Anwar, M.R., O'leary, G., Conyers, M.K., 2014. Managing wheat stubble as an effective approach to sequester soil carbon in a semi-arid environment: spatial modelling. Geoderma 214-215, 50–61. https://doi.org/10.1016/j.geoderma.2013.10.003.

Liu, D.L., Zeleke, K.T., Wang, B., Macadam, I., Scott, F., Martin, R.J., 2017. Crop residue incorporation can mitigate negative climate change impacts on crop yield and improve water use efficiency in a semiarid environment. Eur. J. Agron. 85, 51–68. https://doi.org/10.1016/j.eja.2017.02.004.

Liu, D.L., Zuo, H., 2012. Statistical downscaling of daily climate variables for climate change impact assessment over New South Wales, Australia. Clim. Chang. 115, 629–666. https://doi.org/10.1007/s10584-012-0464-y.

Liu, L., Hao, L., Zhang, Y., Zhou, H., Ma, B., Cheng, Y., Tian, Y., Chang, Z., Zheng, Y., 2022a. The CO2 fertilization effect on leaf photosynthesis of maize (Zea mays L.) depends on growth temperatures with changes in leaf anatomy and soluble sugars. Front. Plant Sci. 13, 890928. https://doi.org/10.3389/fpls.2022.890928.

Liu, Q., Zhang, J., Zhang, H., Yao, F., Bai, Y., Zhang, S., Meng, X., Liu, Q., 2021. Evaluating the performance of eight drought indices for capturing soil moisture dynamics in various vegetation regions over China. Sci. Total Environ. 789, 147803. https://doi.org/10.1016/j.scitotenv.2021.147803.

Liu, S., Xiao, L., Sun, J., Yang, P., Yang, X., Wu, W., 2022b. Probability of maize yield failure increases with drought occurrence but partially depends on local conditions in China. Eur. J. Agron. 139, 126552. https://doi.org/10.1016/j.eja.2022.126552.

Ljung, G.M., Box, G.E., 1978. On a measure of lack of fit in time series models. Biometrika 65, 297–303. https://doi.org/10.1093/biomet/65.2.297.

Malik, A., Li, M., Lenzen, M., Fry, J., Liyanapathirana, N., Beyer, K., Boylan, S., Lee, A., Raubenheimer, D., Geschke, A., Prokopenko, M., 2022. Impacts of climate change and extreme weather on food supply chains cascade across sectors and regions in Australia. Nat. Food 3, 631–643. https://doi.org/10.1038/s43016-022-00570-3.

Mckee, B.T., Doesken, J.N., Kleist, J., 1993. The relationship of drought frequency and duration to time scales. In: Proceedings of the 8th Conference on Applied Climatology, pp. 179–183.
Miguez-Macho, G., Fan, Y., 2021. Spatiotemporal origin of soil water taken up by vegetation. Nature 598, 624–628. https://doi.org/10.1038/s41586-021-03958-6.
Mishra, A.K., Singh, V.P., 2010. A review of drought concepts. J. Hydrol. 391, 202–216. https://doi.org/10.1016/j.jhydrol.2010.07.012.
Mishra, A.K., Singh, V.P., 2011. Drought modeling–a review. J. Hydrol. 403, 157–175. https://doi.org/10.1016/j.jhydrol.2011.03.049.
Mokhtar, A., He, H., Alsafadi, K., Mohammed, S., Ayantobo, O.O., Elbeltagi, A., Abdelwahab, O.M.M., Zhao, H., Quan, Y., Abdo, H.G., Gyasi-Agyei, Y., Li, Y., 2021. Assessment of the effects of spatiotemporal characteristics of drought on crop yields in southwest China. Int. J. Climatol. 42, 3056–3075. https://doi.org/10.1002/joc.7407.
Naseri, K., Hummel, M.A., 2022. A Bayesian copula-based nonstationary framework for compound flood risk assessment along US coastlines. J. Hydrol. 610, 128005. https://doi.org/10.1016/j.jhydrol.2022.128005.
Nóia-Júnior, R.D.S., Ruane, A.C., Athanasiadis, I.N., Ewert, F., Harrison, M.T., Jägermeyr, J., Martre, P., Müller, C., Palosuo, T., Salmerón, M., Webber, H., Maccarthy, D.S., Asseng, S., 2025. Crop models for future food systems. One Earth 8, 101487. https://doi.org/10.1016/j.oneear.2025.101487.
O'neill, B.C., Tebaldi, C., Van Vuuren, D.P., Eyring, V., Friedlingstein, P., Hurtt, G., Knutti, R., Kriegler, E., Lamarque, J.F., Lowe, J., Meehl, G.A., Moss, R., Riahi, K., Sanderson, B.M., 2016. The scenario model intercomparison project (ScenarioMIP) for CMIP6. Geosci. Model. Dev. 9, 3461–3482. https://doi.org/10.5194/gmd-9-3461-2016.
Orlov, A., Jägermeyr, J., Müller, C., Daloz, A.S., Zabel, F., Minoli, S., Liu, W., Lin, T.S., Jain, A.K., Folberth, C., Okada, M., Poschlod, B., Smerald, A., Schneider, J.M., Sillmann, J., 2024. Human heat stress could offset potential economic benefits of CO2 fertilization in crop production under a high-emissions scenario. One Earth 7, 1250–1265. https://doi.org/10.1016/j.oneear.2024.06.012.
Palmer, W.C., 1965. Meteorological Drought. US Weather Bureau, Washington, DC, p. 58. Research paper no. 45.
Peña-Gallardo, M., Vicente-Serrano, S.M., Quiring, S., Svoboda, M., Hannaford, J., Tomas-Burguera, M., Martín-Hernández, N., Domínguez-Castro, F., El Kenawy, A., 2019. Response of crop yield to different time-scales of drought in the United States: spatio-temporal patterns and climatic and environmental drivers. Agric. For. Meteorol. 264, 40–55. https://doi.org/10.1016/j.agrformet.2018.09.019.
Quan, H., Wang, B., Wu, L., Feng, H., Wu, L., Wu, L., Liu, D.L., Siddique, K.H.M., 2024. Impact of plastic mulching and residue return on maize yield and soil organic carbon storage in irrigated dryland areas under climate change. Agric. Ecosyst. Environ. 362. https://doi.org/10.1016/j.agee.2023.108838.
Rahimi-Moghaddam, S., Deihimfard, R., Nazari, M.R., Mohammadi-Ahmadmahmoudi, E., Chenu, K., 2023. Understanding wheat growth and the seasonal climatic characteristics of major drought patterns occurring in cold dryland environments from Iran. Eur. J. Agron. 145, 126772. https://doi.org/10.1016/j.eja.2023.126772.
Rahmati, O., Falah, F., Dayal, K.S., Deo, R.C., Mohammadi, F., Biggs, T., Moghaddam, D. D., Naghibi, S.A., Bui, D.T., 2020. Machine learning approaches for spatial modeling of agricultural droughts in the south-east region of Queensland Australia. Sci. Total Environ. 699, 134230. https://doi.org/10.1016/j.scitotenv.2019.134230.
Rezaei, E.E., Webber, H., Asseng, S., Boote, K., Durand, J.L., Ewert, F., Martre, P., Maccarthy, D.S., 2023. Climate change impacts on crop yields. Nat. Rev. Earth Environ. 4, 831–846. https://doi.org/10.1038/s43017-023-00491-0.
Richetti, J., Lawes, R.A., Whan, A., Gaydon, D.S., Thorburn, P.J., 2024. How well does APSIM NextGen simulate wheat yields across Australia using gridded input data? Validating continental-scale crop model simulations. Eur. J. Agron. 158, 127212. https://doi.org/10.1016/j.eja.2024.127212.
Rosenzweig, C., Jones, J.W., Hatfield, J.L., Ruane, A.C., Boote, K.J., Thorburn, P., Antle, J.M., Nelson, G.C., Porter, C., Janssen, S., Asseng, S., Basso, B., Ewert, F., Wallach, D., Baigorria, G., Winter, J.M., 2013. The Agricultural Model Intercomparison and Improvement Project (AgMIP): protocols and pilot studies. Agric. For. Meteorol. 170, 166–182. https://doi.org/10.1016/j.agrformet.2012.09.011.
Ruane, A.C., Phillips, M., Müller, C., Elliott, J., Jägermeyr, J., Arneth, A., Balkovic, J., Deryng, D., Folberth, C., Iizumi, T., Izaurralde, R.C., Khabarov, N., Lawrence, P., Liu, W., Olin, S., Pugh, T.A.M., Rosenzweig, C., Sakurai, G., Schmid, E., Sultan, B., Wang, X., De Wit, A., Yang, H., 2021. Strong regional influence of climatic forcing datasets on global crop model ensembles. Agric. For. Meteorol. 300, 108313. https://doi.org/10.1016/j.agrformet.2020.108313.
Sahbeni, G., Pleynet, J.B., Jarocki, K., 2023. A spatiotemporal analysis of precipitation anomalies using rainfall Gini index between 1980 and 2022. Atmos. Sci. Lett. 24, e1161. https://doi.org/10.1002/asl.1161.
Sakamoto, Y., Ishiguro, M., Kitagawa, G., 1986. Akaike Information Criterion Statistics, 81. D. Reidel, Dordrecht, The Netherlands, 26853.
Samantaray, A.K., Ramadas, M., Panda, R.K., 2022. Changes in drought characteristics based on rainfall pattern drought index and the CMIP6 multi-model ensemble. Agric. Water Manag. 266, 107568. https://doi.org/10.1016/j.agwat.2022.107568.
Seo, J., Won, J., Lee, H., Kim, S., 2024. Probabilistic monitoring of meteorological drought impacts on water quality of major rivers in South Korea using copula models. Water Res. 251, 121175. https://doi.org/10.1016/j.watres.2024.121175.
Sheffield, J., Goteti, G., Wen, F., Wood, E.F., 2004. A simulated soil moisture based drought analysis for the United States. J. Geophys. Res. Atmos. 109, 1–19. https://doi.org/10.1029/2004jd005182.
Shi, L., Wang, B., Liu, D.L., Feng, P., Cleverly, J., Li, L., Zhang, G., Yu, Q., 2023. Performance of potential evapotranspiration models across different climatic stations in New South Wales, Australia. J. Hydrol. Reg. Stud. 50, 101573. https://doi.org/10.1016/j.ejrh.2023.101573.
Simanjuntak, C., Gaiser, T., Ahrends, H.E., Ceglar, A., Singh, M., Ewert, F., Srivastava, A. K., 2023. Impact of climate extreme events and their causality on maize yield in South Africa. Sci. Rep. 13, 12462. https://doi.org/10.1038/s41598-023-38921-0.
Slater, L.J., Huntingford, C., Pywell, R.F., Redhead, J.W., Kendon, E.J., 2022. Resilience of UK crop yields to compound climate change. Earth Syst. Dyn. 13, 1377–1396. https://doi.org/10.5194/esd-13-1377-2022.
Spinoni, J., Barbosa, P., De Jager, A., Mccormick, N., Naumann, G., Vogt, J.V., Magni, D., Masante, D., Mazzeschi, M., 2019. A new global database of meteorological drought events from 1951 to 2016. J. Hydrol. Reg. Stud. 22, 100593. https://doi.org/10.1016/j.ejrh.2019.100593.
Steensen, B.M., Myhre, G., Hodnebrog, Ø., Fischer, E., 2025. Future increase in European compound events where droughts end in heavy precipitation. NPJ Clim. Atmos. Sci. 8, 267. https://doi.org/10.1038/s41612-025-01139-0.
Stenson, M., Searle, R., Malone, B., Sommer, A., Renzullo, L., Di, H., 2021. Australia wide daily volumetric soil moisture estimates. Version 1.0. Terr. Ecosyst. Res. Netw. 1, 1. https://doi.org/10.25901/b020-nm39.
Sugiura, D., Wang, Y., Kono, M., Mizokami, Y., 2024. Exploring the responses of crop photosynthesis to CO2 elevation at the molecular, physiological, and morphological levels toward increasing crop production. Crop Environ. 3, 75–83. https://doi.org/10.1016/j.crope.2023.11.006.
Sun, H., Wang, Y., Wang, L., 2024. Impact of climate change on wheat production in China. Eur. J. Agron. 153, 127066. https://doi.org/10.1016/j.eja.2023.127066.
Sun, W., Fleisher, D., Timlin, D., Ray, C., Wang, Z., Sahila, B., Reddy, V., 2023. Does drought stress eliminate the benefit of elevated CO2 on soybean yield? Using an improved model to link crop and soil water relations. Agric. For. Meteorol. 343, 109747. https://doi.org/10.1016/j.agrformet.2023.109747.
Sweet, L.B., Athanasiadis, I.N., Van Bree, R., Castellano, A., Martre, P., Paudel, D., Ruane, A.C., Zscheischler, J., 2025. Transdisciplinary coordination is essential for advancing agricultural modeling with machine learning. One Earth 8, 101233. https://doi.org/10.1016/j.oneear.2025.101233.
Tan, Z., De Voil, P., Zhao, J., Zhao, D., Mcgowan, H., Xiao, L., Rodriguez, D., 2025. Pathways towards net zero emissions in grain cropping farms. Agric. Syst. 229, 104401. https://doi.org/10.1016/j.agsy.2025.104401.
Tardieu, F., Simonneau, T., Muller, B., 2018. The physiological basis of drought tolerance in crop plants: a scenario-dependent probabilistic approach. Annu. Rev. Plant Biol. 69, 733–759. https://doi.org/10.1146/annurev-arplant-042817-040218.
Tefera, M.L., Seddaiu, G., Carletti, A., Awada, H., 2024. Rainfall variability and drought in West Africa: challenges and implications for rainfed agriculture. Theor. Appl. Climatol. 156, 1–21. https://doi.org/10.1007/s00704-024-05251-8.
Temizhan, E., Mirtagioglu, H., Mendes, M., 2022. Which correlation coefficient should be used for investigating relations between quantitative variables? Am. Acad. Sci. Res. J. Eng. Technol. Sci. 85, 265–277.
Terrer, C., Jackson, R.B., Prentice, I.C., Keenan, T.F., Kaiser, C., Vicca, S., Fisher, J.B., Reich, P.B., Stocker, B.D., Hungate, B.A., Peñuelas, J., Mccallum, I., Soudzilovskaia, N.A., Cernusak, L.A., Talhelm, A.F., Van Sundert, K., Piao, S., Newton, P.C.D., Hovenden, M.J., Blumenthal, D.M., Liu, Y.Y., Müller, C., Winter, K., Field, C.B., Viechtbauer, W., Van Lissa, C.J., Hoosbeek, M.R., Watanabe, M., Koike, T., Leshyk, V.O., Polley, H.W., Franklin, O., 2019. Nitrogen and phosphorus constrain the CO2 fertilization of global plant biomass. Nat. Clim. Chang. 9, 684–689. https://doi.org/10.1038/s41558-019-0545-2.
Tian, L., Yuan, S., Quiring, S.M., 2018. Evaluation of six indices for monitoring agricultural drought in the south-central United States. Agric. For. Meteorol. 249, 107–119. https://doi.org/10.1016/j.agrformet.2017.11.024.
Verburg, K., Cocks, B., Manning, B., Truman, G., Schwenke, G., 2017. APSoil Plant Available Water Capacity (PAWC) Characterisation of Select Liverpool Plains Soils and Their Landscape Context. CSIRO, Australia.
Vergni, L., Vinci, A., Todisco, F., 2021. Effectiveness of the new standardized deficit distance index and other meteorological indices in the assessment of agricultural drought impacts in central Italy. J. Hydrol. 603, 126986. https://doi.org/10.1016/j.jhydrol.2021.126986.
Vicente-Serrano, S.M., Beguería, S., López-Moreno, J.I., 2010. A multiscalar drought index sensitive to global warming: the standardized precipitation evapotranspiration index. J. Clim. 23, 1696–1718. https://doi.org/10.1175/2009jcli2909.1.
Virgilio, G.D., Ji, F., Tam, E., Nishant, N., Evans, J.P., Thomas, C., Riley, M.L., Beyer, K., Grose, M.R., Narsey, S., Delage, F., 2022. Selecting CMIP6 GCMs for CORDEX dynamical downscaling: model performance, independence, and climate change signals. Earths Future 10. https://doi.org/10.1029/2021ef002625, 2021EF002625.
Wable, P.S., Jha, M.K., Shekhar, A., 2018. Comparison of drought indices in a semi-arid river basin of India. Water Resour. Manag. 33, 75–102. https://doi.org/10.1007/s11269-018-2089-z.
Wan, W., Liu, Z., Li, K., Wang, G., Wu, H., Wang, Q., 2021. Drought monitoring of the maize planting areas in Northeast and North China Plain. Agric. Water Manag. 245, 106636. https://doi.org/10.1016/j.agwat.2020.106636.
Wang, B., Feng, P., Liu, L., O'leary, G.J., Macadam, I., Waters, C., Asseng, S., Cowie, A., Jiang, T., Xiao, D., Ruan, H., He, J., Yu, Q., 2020. Sources of uncertainty for wheat yield projections under future climate are site-specific. Nat. Food 1, 720–728. https://doi.org/10.1038/s43016-020-00181-w.
Wang, B., Jägermeyr, J., O'leary, G.J., Wallach, D., Ruane, A.C., Feng, P., Li, L., Liu, D.L., Waters, C., Yu, Q., Asseng, S., Rosenzweig, C., 2024a. Pathways to identify and reduce uncertainties in agricultural climate impact assessments. Nat. Food. https://doi.org/10.1038/s43016-024-01014-w.
Wang, B., Li, L., Feng, P., Chen, C., Luo, J.J., Taschetto, A.S., Harrison, M.T., Liu, K., Liu, D.L., Yu, Q., Guo, X., 2024b. Probabilistic analysis of drought impact on wheat

yield and climate change implications. Weather Clim. Extrem. 45, 100708. https://doi.org/10.1016/j.wace.2024.100708.
Wang, B., Liu, D.L., Asseng, S., Macadam, I., Yang, X., Yu, Q., 2017a. Spatiotemporal changes in wheat phenology, yield and water use efficiency under the CMIP5 multimodel ensemble projections in eastern Australia. Clim. Res. 72, 83–99. https://doi.org/10.3354/cr01458.
Wang, B., Liu, D.L., Asseng, S., Macadam, I., Yu, Q., 2017b. Modelling wheat yield change under CO2 increase, heat and water stress in relation to plant available water capacity in eastern Australia. Eur. J. Agron. 90, 152–161. https://doi.org/10.1016/j.eja.2017.08.005.
Wang, B., Liu, L., O'leary, G.J., Asseng, S., Macadam, I., Lines-Kelly, R., Yang, X., Clark, A., Crean, J., Sides, T., Xing, H., Mi, C., Yu, Q., 2018. Australian wheat production expected to decrease by the late 21st century. Glob. Chang. Biol. 24, 2403–2415. https://doi.org/10.1111/gcb.14034.
Wang, B., Waters, C., Anwar, M.R., Cowie, A., Liu, L., Summers, D., Paul, K., Feng, P., 2022a. Future climate impacts on forest growth and implications for carbon sequestration through reforestation in southeast Australia. J. Environ. Manag. 302, 113964. https://doi.org/10.1016/j.jenvman.2021.113964.
Wang, E., He, D., Luo, Z., 2019. Predicting soil water holding capacity from climate and crop yield. In: Proceedings of the 2019 Agronomy Australia Conference. Wagga Wagga, Australia.
Wang, Z., Wang, C., Liu, S., 2022b. Elevated CO2 alleviates adverse effects of drought on plant water relations and photosynthesis: a global meta-analysis. J. Ecol. 110, 2836–2849. https://doi.org/10.1111/1365-2745.13988.
Wei, Q., Pan, H., Yang, Y., Tan, S., Zheng, L., Wang, H., Zhang, J., Zhang, Z., Wei, Y., Wang, X., Ma, X., Xiong, S., 2023a. Effects of elevated atmospheric [CO(2)] on grain starch characteristics in different specialized wheat. Front. Plant Sci. 14, 1334053. https://doi.org/10.3389/fpls.2023.1334053.
Wei, X., Huang, S., Jianfeng, Huang, Q., Leng, G., Liu, D., Guo, W., Zheng, X., Bai, Q., 2023b. The negative-positive feedback transition thresholds of meteorological drought in response to agricultural drought and their dynamics. Sci. Total Environ. 906, 167817. https://doi.org/10.1016/j.scitotenv.2023.167817.
Wen, P., Wei, Q., Zheng, L., Rui, Z., Niu, M., Gao, C., Guan, X., Wang, T., Xiong, S., 2023. Adaptability of wheat to future climate change: effects of sowing date and sowing rate on wheat yield in three wheat production regions in the North China Plain. Sci. Total Environ. 901, 165906. https://doi.org/10.1016/j.scitotenv.2023.165906.
White, H., 1982. Maximum likelihood estimation of misspecified models. Econom. J. Econom. Soc. 1982, 1–25. https://doi.org/10.2307/1912526.
Wu, H., Su, X., Huang, S., Singh, V.P., Zhou, S., Tan, X., Hu, X., 2025. Decreasing dynamic predictability of global agricultural drought with warming climate. Nat. Clim. Chang. 15, 411–419. https://doi.org/10.1038/s41558-025-02289-y.
Wu, H., Su, X., Singh, V.P., Feng, K., Niu, J., 2021. Agricultural drought prediction based on conditional distributions of vine copulas. Water Resour. Res. 57. https://doi.org/10.1029/2021wr029562 e2021WR029562.
Xiang, K., Wang, B., Liu, D.L., Chen, C., Ji, F., Yang, Y., Li, S., Huang, M., Huete, A., Yu, Q., 2025. Soil with high plant available water capacity can mitigate the risk of wheat growth under drought conditions in southeastern Australia. Eur. J. Agron. 164, 127460. https://doi.org/10.1016/j.eja.2024.127460.
Xiang, K., Wang, B., Liu, D.L., Chen, C., Ji, F., Yao, S., Li, S., Huete, A., Li, Y., Yu, Q., 2026. Future climate change increases the risk of wheat yield loss due to agricultural drought in southeastern Australia. Eur. J. Agron. 173, 127909. https://doi.org/10.1016/j.eja.2025.127909.
Xiang, K., Wang, B., Liu, D.L., Chen, C., Waters, C., Huete, A., Yu, Q., 2023. Probabilistic assessment of drought impacts on wheat yield in south-eastern Australia. Agric. Water Manag. 284, 108359. https://doi.org/10.1016/j.agwat.2023.108359.
Yang, C., Liu, C., Liu, Y., Gao, Y., Xing, X., Ma, X., 2024. Prediction of drought trigger thresholds for future winter wheat yield losses in China based on the DSSAT-CERES-wheat model and Copula conditional probabilities. Agric. Water Manag. 299, 108881. https://doi.org/10.1016/j.agwat.2024.108881.
Yao, N., Li, Y., Liu, Q., Zhang, S., Chen, X., Ji, Y., Liu, F., Pulatov, A., Feng, P., 2022. Response of wheat and maize growth-yields to meteorological and agricultural droughts based on standardized precipitation evapotranspiration indexes and soil moisture deficit indexes. Agric. Water Manag. 266, 107566. https://doi.org/10.1016/j.agwat.2022.107566.
Yao, S., Liu, D.L., Wang, B., Webb, J.K., Li, S., Huete, A., Xiang, K., Yu, Q., 2026. Climate warming enhances sugarcane yield and increases annual harvest frequency in northern coastal New South Wales, Australia. Agric. Syst. 231, 104502. https://doi.org/10.1016/j.agsy.2025.104502.
Ye, Z., Qiu, X., Chen, J., Cammarano, D., Ge, Z., Ruane, A.C., Liu, L., Tang, L., Cao, W., Liu, B., Zhu, Y., 2020. Impacts of 1.5 °C and 2.0 °C global warming above pre-industrial on potential winter wheat production of China. Eur. J. Agron. 120, 126149. https://doi.org/10.1016/j.eja.2020.126149.
Yerdelen, C., Abdelkader, M., Eris, E., 2021. Assessment of drought in SPI series using continuous wavelet analysis for Gediz Basin, Turkey. Atmos. Res. 260, 105687. https://doi.org/10.1016/j.atmosres.2021.105687.
Yuan, C., Yamagata, T., 2015. Impacts of IOD, ENSO and ENSO Modoki on the Australian winter wheat yields in recent decades. Sci. Rep. 5, 17252. https://doi.org/10.1038/srep17252.
Zargar, A., Sadiq, R., Naser, B., Khan, F.I., 2011. A review of drought indices. Environ. Rev. 19, 333–349. https://doi.org/10.1139/a11-013.
Zeleke, K., 2021. Simulating agronomic adaptation strategies to mitigate the impacts of climate change on wheat yield in South-Eastern Australia. Agronomy 11, 337. https://doi.org/10.3390/agronomy11020337.
Zhang, C., Wang, Y., Jia, X., Shao, M.A., An, Z., 2020. Variations in capacity and storage of plant-available water in deep profiles along a revegetation and precipitation gradient. J. Hydrol. 581. https://doi.org/10.1016/j.jhydrol.2019.124401.
Zhang, Y., Hao, Z., Feng, S., Zhang, X., Hao, F., 2023a. Changed relationship between compound dry-hot events and ENSO at the global scale. J. Hydrol. 621, 129559. https://doi.org/10.1016/j.jhydrol.2023.129559.
Zhang, Z., Li, Y., Chen, X., Wang, Y., Niu, B., Liu, D.L., He, J., Pulatov, B., Hassan, I., Meng, Q., 2023b. Impact of climate change and planting date shifts on growth and yields of double cropping rice in southeastern China in future. Agric. Syst. 205, 103581. https://doi.org/10.1016/j.agsy.2022.103581.
Zhao, W., Yang, M., Yu, G., Chen, Z., Wang, Q., 2023. The temporal response of soil respiration to environment differed from that on spatial scale. Agric. For. Meteorol. 342, 109752. https://doi.org/10.1016/j.agrformet.2023.109752.
Zheng, B., Chenu, K., Doherty, A., Chapman, S., 2015. The APSIM-wheat module.
Zheng, J., Zhang, S., 2025. Decomposing the total uncertainty in wheat modeling: an analysis of model structure, parameters, weather data inputs, and squared bias contributions. Agric. Syst. 224, 104215. https://doi.org/10.1016/j.agsy.2024.104215.
Zhu, C., Wolf, J., Zhang, J., Anderegg, W.R.L., Bunce, J.A., Ziska, L.H., 2023. Rising temperatures can negate CO2 fertilization effects on global staple crop yields: a meta-regression analysis. Agric. For. Meteorol. 342, 109737. https://doi.org/10.1016/j.agrformet.2023.109737.